ACS OMEGA

http://pubs.acs.org/journal/acsodf

Article

Antioxidative-, Antimicrobial-, Enzyme Inhibition-, and Cytotoxicity-Based Fractionation and Isolation of Active Components from *Monotheca buxifolia* (Falc.) A. DC. Stem Extracts

Joham Sarfraz Ali, Naheed Riaz, Abdul Mannan, Saira Tabassum, and Muhammad Zia*

Cite This: *ACS Omega* 2022, 7, 3407−3423

Read Online

ACCESS | Metrics & More | Article Recommendations

ABSTRACT: The current study elaborates the pharmacological potential of the methanolic extract and its fractions of the stems of *Monotheca buxifolia* based on thin-layer chromatography and column chromatography analyses, exploiting biological and phytochemical assays. The results suggest that bioassay-guided isolation and fractionation led to the accumulation of biologically active components in the most active fractions that resulted in the isolation of different compounds. Structural elucidation of the purified compounds was accomplished using spectroscopic one-dimensional (^{1}H, ^{13}C) and two-dimensional NMR (heteronuclear multiple quantum coherence, heteronuclear multiple bond coherence, and correlation spectroscopy) and spectrometric (electron ionization mass spectrometry and high-resolution electron ionization mass spectrometry) techniques. The *n*-hexane, $CHCl_3$, and EtAOc fractions led to the isolation of lupeol from different fractions. 1-Triacontanol was also isolated from the *n*-hexane fraction, while benzoic acid, methyl benzoate, ursolic acid, and 3-hydroxybenzoic acid were obtained from the EtOAc fraction. The compounds depicted good-to-moderate total antioxidative potential and total reducing power activity and significant free-radical scavenging activity. All the compounds showed significant urease and lipase inhibitory activity with poor-to-moderate amylase inhibition. Significant zone of inhibition was observed against different bacterial strains by the isolated compounds. This work therefore states that bioassay-guided isolation plays a vital role in the isolation of biologically active constituents that can be exploited for drug development.

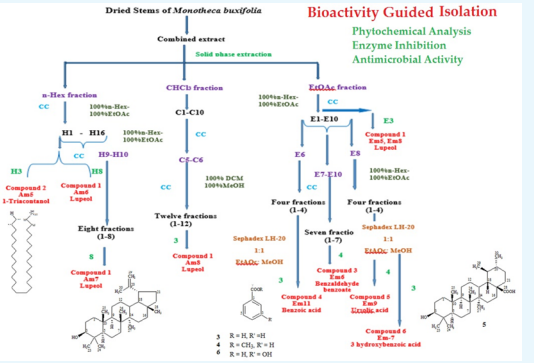

INTRODUCTION

Since the commencement of human existence, man has accustomed himself to plants and used them accordingly. In search of food and to accommodate the human sufferings, man began to differentiate medicinal plants from the ones possessing pharmacological action.[1] Medicinal plants are perceived as inherent drug aspirants as they have drug-like characteristics.[2] Due to the ample geographical distribution of ethnobotanically significant medicinal plants, nutraceuticals cater equivocal promise for novel drug discovery.[3] Medicinal plants are scrutinized globally due to the higher yield of pharmacologically active compounds, antioxidative potential, therapeutic tendency, economic viability, and safety.[4] Medicinal plants are enriched sources of secondary metabolites (alkaloids, flavonoids, saponins, terpenoids, steroids, glycosides, tannins, volatile oils, etc.) acting as potent free-radical scavenging agents that are directly correlated to their antioxidant potential.[5] Phytochemicals, on the other hand, are also well known for their key role against several human diseases.[6] However, lack of knowledge transfer and debasement regarding the role of active agents have caused the abrogation of pre-existing ethnobotanical data.[7] Bioassay-guided isolation is the most effective way as it scrutinizes the eminent aliquots among all, simplifying the process that leads to the isolation of pure and active compounds.[8]

Sapotaceae family is renowned for edible fruits and comprises approx. 800 species and 65 genera. *Monotheca buxifolia* (Gurguri) is a member of this family that is found in dry hilly areas. It is found in South Asia (Pakistan, India, and Afghanistan) and Middle East [Iran, Qatar, Saudi Arabia, Iraq, and United Arab Emirates (UAE)]. In Pakistan, it is distributed in Chitral, Kohat, Loralai, Zhob, Drosh, Gorakh Hills, Kala Chitta Hills, Attock District, Darra-Adamkhel, and Mohmand Agency.[9] The plant is extolled due to its efficacious tendency against urinary, liver, and kidney diseases. It is also known as laxative, anticancer, hepatoprotective, analgesic, digestive, and antipyretic agents.[10,11] Literature identifies the antioxidant,[12]

Received: October 9, 2021
Accepted: December 21, 2021
Published: January 18, 2022

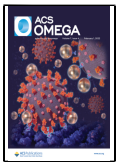

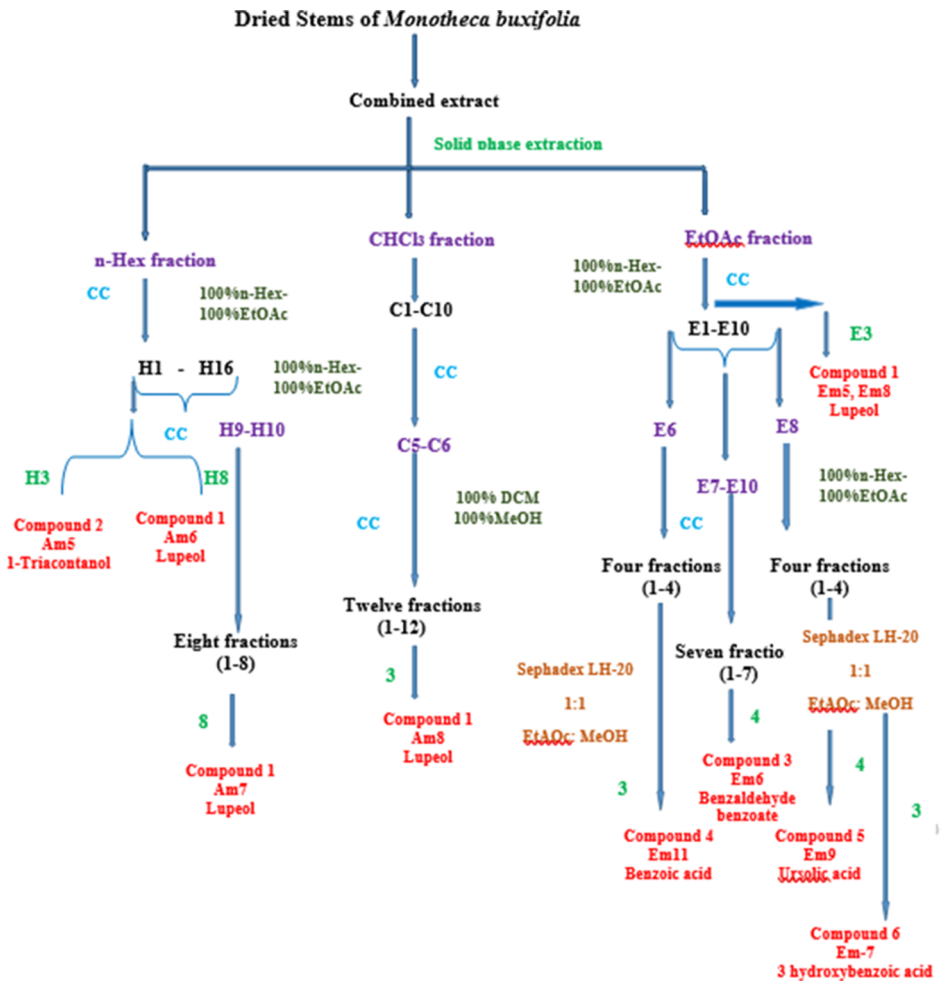

Figure 1. Schematic representation of *M. buxifolia* stem fractions and isolation of compounds.

anti-inflammatory and antipyretic,[13,14] renal protective,[15] and antimicrobial[16] potential of the leaves and fruits of this plant. UHPLC−MS analysis of *M. buxifolia* extracts has shown the presence of polygalacin D, diosgenin, robinin, kaempferol, 3-*O*-*cis*-coumaroyl maslinic acid, and lucidumol A. Catechin, rutin, and epicatechin have also been identified using high-performance liquid chromatography coupled with photodiode array detection (HPLC-PDA) analysis in different plant parts.[17] Recently, bioactivity-guided isolation resulted in the crystallization of lupeol as the major active ingredient.[18]

The current study was formulated to validate the pharmacological potential of the stem extract, fractions, and re-fractions of *M. buxifolia* using an array of biological assays, thin-layer chromatography (TLC), and column chromatography (CC). The lead compounds having biological activity were also identified using these tools. The purpose of the current study was to identify the phytochemicals, antioxidants, enzyme inhibition, antifungal, antibacterial, and cytotoxic potential of extracts, and fractions and re-fractions of the stems of *M. buxifolia* in a schematized way, mapping the way toward bioassay-guided isolation of lead compounds.

RESULTS AND DISCUSSION

The studies performed on *M. buxifolia* suggest its diverse biological potential and phytochemical assortment.[19] Despite the use of modern isolation and identification techniques, the conventional method of detection and isolation is still more reliable and has its unique position. The bioassay-guided isolation and fractionation method identifies the biological potential of the extracts being targeted, and after each fractionation, the steps pave the way for the isolation of active constituents responsible for those activities. This study focused on crude extraction from *M. buxifolia* stems that were fractionated polarity-wise using CC, and fractions were combined keeping in view their bands obtained during TLC analysis and the biological activities of fractions. The methodology continued until notable activity was observed in fractions or a compound was isolated.

The fractions *n*-hexanes, $CHCl_3$, and EtOAc were subjected to CC independently. The *n*-hexane fraction resulted in H1−H16 fractions, and two compounds were crystallized, one in H8 fraction was separated (AM-6) and one in H3 fraction was separated (AM-5). The $CHCl_3$ fraction resulted in C1−C10 fractions, and on the basis of TLC analysis, C5−C6 were subjected to re-separation using CC. The combined C5−C6 fractions resulted in further 12 fractions (1−12). From the 3rd fraction of C5−C6, one compound was crystallized (AM-8). The EtOAc extract produced fractions E1−E10; two compounds (lupeol in both) were crystallized in the E3 fraction (EM-8 and EM-5), and based on TLC analysis, E6, E8, E7, E9, and E10 were subjected to CC. E6 ended with further four (1−4) fractions, and from the 3rd fraction, one compound was isolated (EM-11). E7, E9, and E10 (in combination) ended with seven (1−7) fractions, and among them, one compound (EM-

https://doi.org/10.1021/acsomega.1c05647
ACS Omega 2022, 7, 3407−3423

6) was crystallized from the 4th fraction. E8 chromatography resulted in fractions 1−4. The 4th fraction, when processed on Sephadex LH-20, produced isolation of the EM-9 compound, and the 3rd fraction processed similar to that of the 4th, resulting in the EM-7 compound (Figure 1).

CC is known to separate active components on the basis of polarity and differential solubility of compounds. TLC profiling acted as a starting clue for the detection, occurrence, and isolation of significant phytochemicals.[20] TLC profiling facilitates a better understanding of the nature, polarity, and specific class of the compounds being isolated from the extract or fraction.[21]

Biological and Phytochemical Activities of Fractions. The biological evaluation of initial fractions (*n*-hexane, $CHCl_3$, and EtOAc) showed that the EtOAc fraction contained the maximum amount of 60.3 ± 1.9 and 29.8 ± 1.6 μg/mg extract for phenolics and flavonoids, respectively (Table 1).

Table 1. Phytochemical and Biological Activities of Fractions of *M. buxifolia* Stem Extract

fractions	*n*-hexane	$CHCl_3$	EtOAc
Phytochemical Analysis			
TPC μgQE/mg extract	9.7 ± 1.7	15.7 ± 1.6	60.3 ± 1.9
TFC μgGAE/mg extract	4.5 ± 0.9	12.4 ± 1.3	29.8 ± 1.6
TAC μgAAE/mg extract	12.2 ± 1.9	32.0 ± 1.7	79.4 ± 1.5
TRP μgAAE/mg extract	16.7 ± 1.2	33.8 ± 1.8	99.3 ± 2.6
DPPH %	20.9 ± 1.6	48.7 ± 2.2	70.8 ± 2.4
Enzyme Inhibition (%)			
amylase	19.7 ± 1.2	17.2 ± 0.8	10.8 ± 1.1
urease	87.6 ± 2.5	85.6 ± 2.3	49.5 ± 2.1
lipase	41.5 ± 1.9	63.1 ± 1.9	22.7 ± 1.6
Toxicity Assays			
PK (bald zone), mm	7 ± 0.5	7 ± 1.4	7 ± 1.2
PK (clear zone), mm			
brine shrimp LD_{50}, μg/mL	86.5	56.1	55.5
antileishmanial %	70 ± 1.4	75 ± 1.1	
Antibacterial Activity (ZOI, mm)			
E. coli			
P. aeruginosa	6 ± 0.7	6 ± 0.6	12 ± 0.9
K. pneumoniae	8 ± 1.0	15.5 ± 1.5	
B. subtilis	12 ± 1.1	18 ± 1.3	19 ± 1.7
S. aureus		8 ± 0.7	8 ± 0.6
Antifungal Activity (ZOI, mm)			
A. niger	12 ± 0.8	10 ± 0.5	12 ± 0.6
F. solani	20 ± 1.4	20 ± 0.9	20 ± 1.6
M. species	14 ± 1.2	10 ± 0.8	
A. fumigatus	18 ± 1.3	18 ± 0.9	20 ± 0.6
A. flavus	18 ± 0.7	14 ± 1.0	12 ± 0.8

The antioxidant activities [TAC, TRP, and 2,2-diphenyl-1-picrylhydrazyl (DPPH)] were also observed to be significantly higher in EtOAc fractions. All the three fractions did not show promising amylase inhibition activity, but prominent urease inhibition was observed by *n*-hexane (87.6%) and $CHCl_3$ (85.6%) fractions. The $CHCl_3$ fraction also showed significant lipase inhibition (63.1%) (Table 1). All the fractions did not show good protein kinase inhibition activity. Brine shrimp toxicity assay revealed that the EtAOC fraction had an LD_{50} value of 55.5 μg/mL compared to $CHCl_3$ and *n*-hexane fractions. Significant antileishmanial activity was observed in $CHCl_3$ and *n*-hexane fractions (75 and 70% mortality, respectively). EtOAc, *n*-hexane, and $CHCl_3$ fractions showed promising zone of inhibition (ZOI) of 18, 12 and 19 mm, respectively, against *Bacillus subtilis*. EtAOc and $CHCl_3$ fractions were also active against *Pseudomonas aeruginosa* and *Klebsiella pneumoniae,* with ZOI of 12 and 15.5 mm, respectively. Table 1 shows that all the fractions showed significant antifungal activity against the tested fungal strains. All the fractions were most active against *Fusarium solani* that showed ZOI of 20 mm. EtAOc also showed activity against *Aspergillus. fumigates,* with ZOI of 20 mm.

Total Phenolics and Flavonoid Contents. Phenolics belong to the class of secondary metabolites having a marked role in stress (oxidative), cell death, and cytotoxicity by retrieving and nullifying free radicals or by chelating with trace elements that later facilitates the antioxidant defense system of living entities.[22] The antioxidant potential of phenols is associated to the occurrence of hydroxyl, methoxy, and ketonic groups and double-bond conjugation within the phenolic molecule directing it to polyphenolic entities (flavonoids, tannins, and phenolic acids).[23]

The *n*-hexane fractions (H1−H16) of the branches obtained during CC depicted the highest phenolic content in H11 and flavonoid content in H16, that is, 49.3 ± 0.9 GAE/mg extract and 34.3 ± 1.5 μg QE/mg extract, respectively (Figure 2A). The *n*-hexane fractions H9−H10 were combined and subjected to another column, resulting in eight fractions (1−8); among them, the highest phenol and flavonoid contents of 46.2 ± 1.5 μg GAE/mg extract and 41.0 ± 0.5 μg QE/mg, respectively, were observed in the 3rd fraction (Figure 2B).

The highest phenolic and flavonoid contents for the chloroform ($CHCl_3$) fraction were present in C9 (50.2 ± 1.4 μg GAE/mg extract and 21.9 ± 1.4 μg QE/mg extract, respectively) (Figure 3A). Later, the fractions C5−C6 were combined in TLC analysis and on the basis of the second highest position in terms of the phenolic content (30 ± 1.4 μg GAE/mg extract) and were subjected to CC. This column resulted in 12 fractions (1−12) that were further tested for the highest phenolic and flavonoid contents, and the highest values were observed in the 6th fraction depicting 86.9 ± 1.5 μg GAE/mg extract and 49.7 ± 0.5 μg QE/mg extract, respectively, as shown in Figure 3B. An increase in the activity of the phenolics and flavonoids was observed after the fractionation process that is directly linked with the purification of these fractions.

Among EtOAc fractions, E10 showed the highest phenolic and flavonoid contents, that is, 81.5 ± 1.7 μg GAE/mg extract and 68.9 ± 1.5 μg QE/mg extract, respectively (Figure 4A). E6 fraction of EtAOc further fractionated in four fractions (1−4) by CC. Among them, the 4th fraction represented the maximum phenolic and flavonoid contents of 39.0 ± 0.7 μg GAE/mg extract and 20.3 ± 1.4 μg QE/mg extract, respectively, as shown in Figure 4B. E7−E10 excluding E8 were combined based on the TLC pattern and again subjected to CC. This resulted in seven fractions (1−7), and the highest phenolic and flavonoid contents were observed in the 6th fraction, that is, 49.2 ± 1.5 μg GAE/mg extract and 39.6 ± 0.5 μg QE/mg extract, respectively (Figure 4C). The E8 column resulted in four fractions (1−4), and the maximum phenolic and flavonoid potentials were observed in the 4th fraction, that is, 30.5 ± 0.9 μg GAE/mg extract and 18.5 ± 1.9 μg QE/mg extract, respectively (Figure 4D).

The phytochemicals are inclined and soluble in polar solvents in comparison to nonpolar solvents, and by looking at the results, it is evident that EtOAc fractions depicted higher phenolic and flavonoid contents in comparison to *n*-hexane and

https://doi.org/10.1021/acsomega.1c05647
ACS Omega 2022, 7, 3407−3423

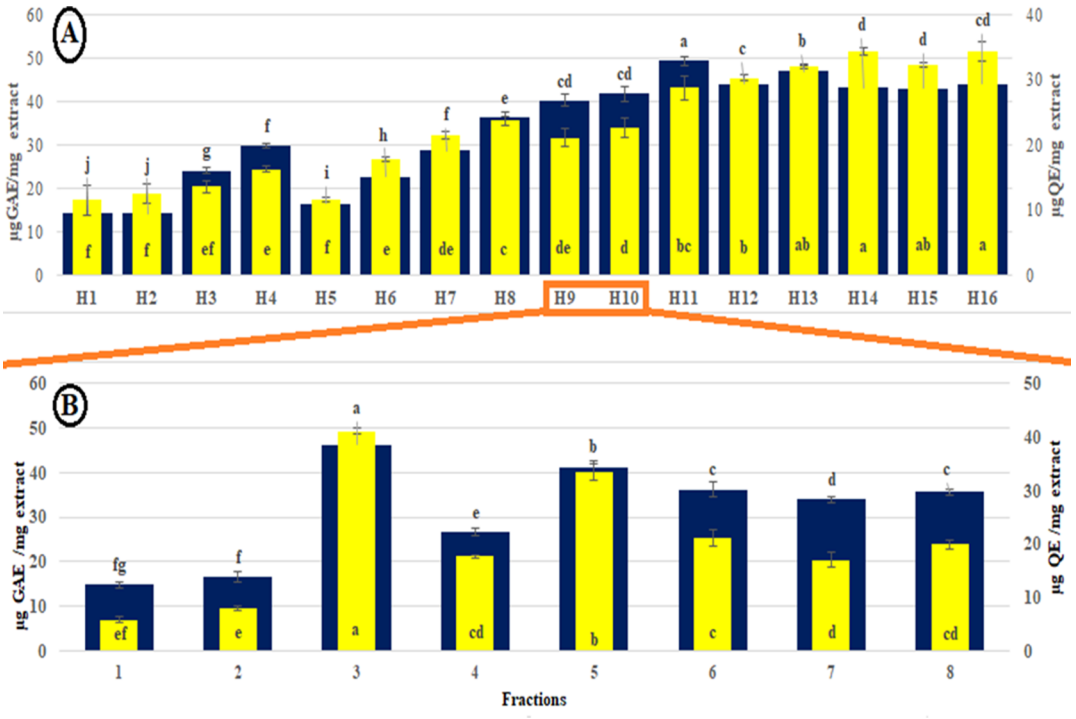

Figure 2. Phytochemical analysis of *n*-hexane fractions. (A) TPC and TFC of H1−H16 of the *n*-hexane fraction; (B) TPC and TFC of 1−8 of H9−H10 fractions.

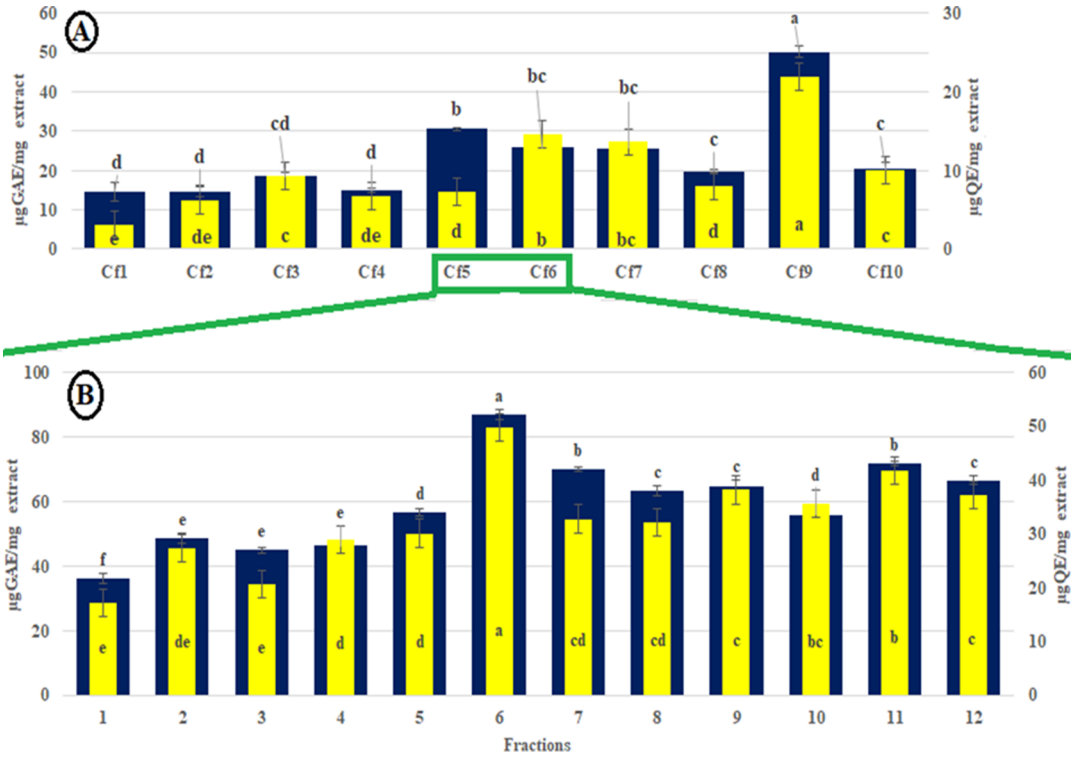

Figure 3. TPC and TFC of $CHCl_3$ fractions of *M. buxifolia* stem. (A)TPC and TFC of C1−C10 fractions. (B) TPC and TFC of 1−12 subfractions of C5−C6 fractions.

$CHCl_3$.[24] The results obtained are in accordance to the previous work performed supporting the polar nature of phenolics and flavonoids.[25] Phenolics are considered the antioxidants occurring naturally and having the capability to donate hydrogen atoms to stabilize them in return. This tendency is linked to the aromatic nature and the hydroxyl substituents present within these. However, flavonoids, a subclass of phenols, have the antioxidant tendency due to the hydroxyl group (phenolic). They are recognized for their ion chelating tendency and delaying or inhibiting the oxidation process by hindering the oxidative chain reaction.[26]

https://doi.org/10.1021/acsomega.1c05647
ACS Omega 2022, 7, 3407−3423

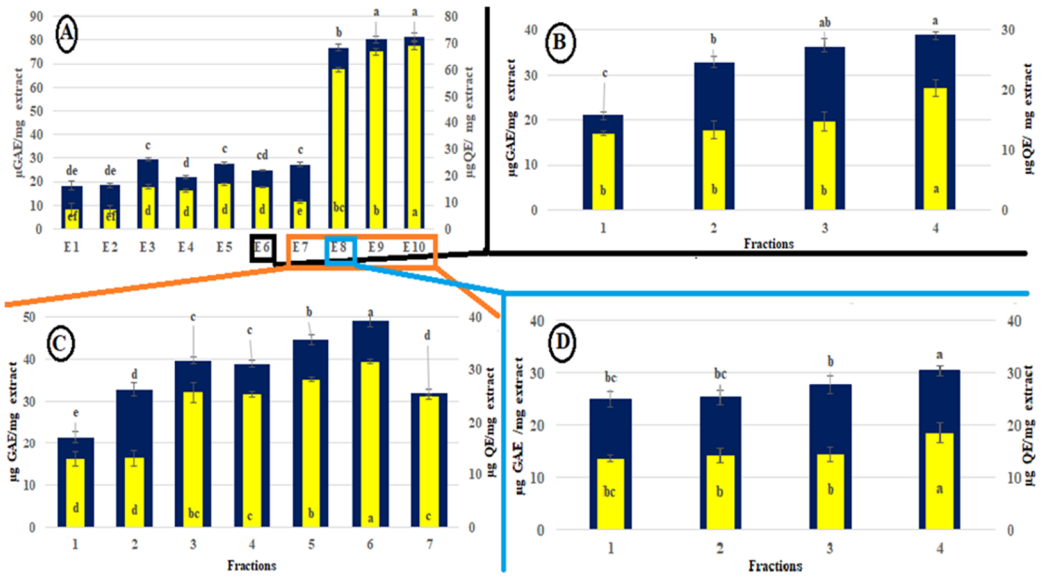

Figure 4. TPC and TFC of EtOAc fractions of *M. buxifolia* stem. (A) TPC and TFC of E1−E10 fractions. (B) TPC and TFC of 1−4 subfractions of the E6 fraction. (C) TPC and TFC of 1−7 subfractions of E7, E9, and E10 (in combination) fractions. (D) TPC and TFC of 1−4 subfractions of E8 of EtOAc fractions.

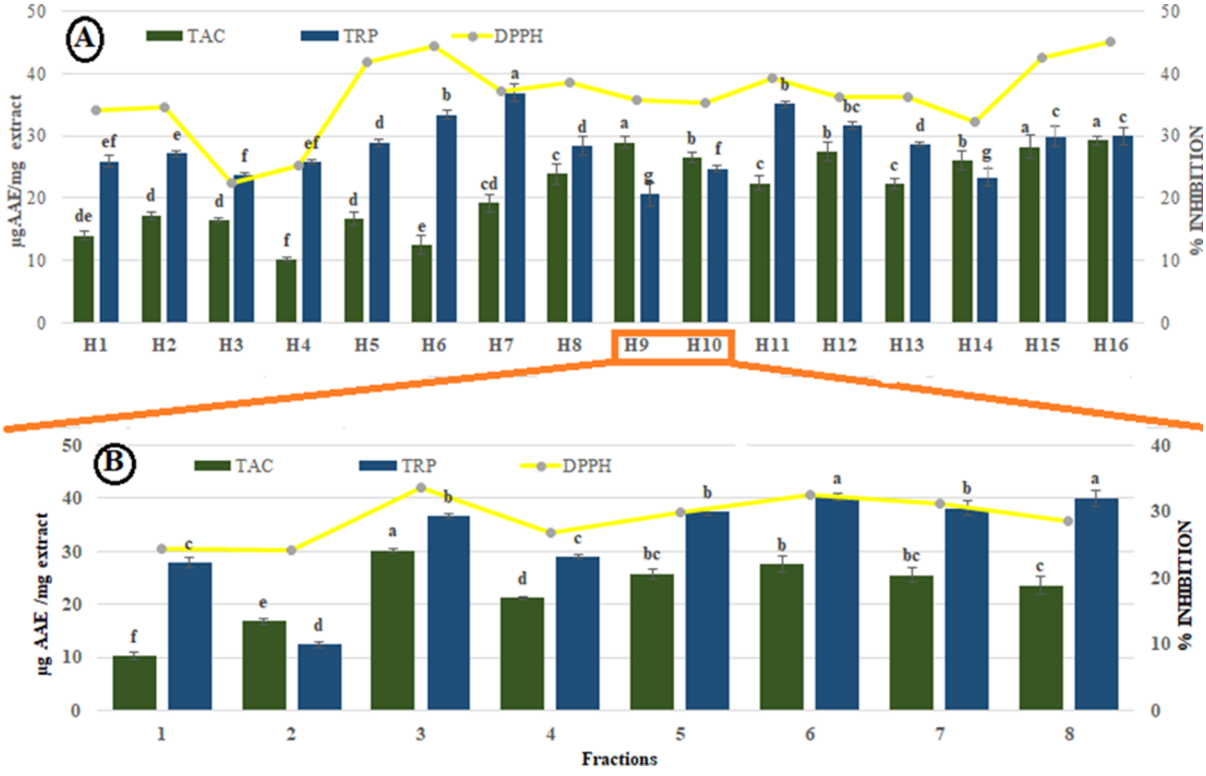

Figure 5. Antioxidant assays of *n*-hexane fractions. (A) TAC, TRP, and DPPH of H1−H16 of the *n*-hexane fraction. (B) TAC, TRP, and DPPH of 1−8 of H9−H10 fractions.

Antioxidant Evaluation. In order to confirm the antioxidant potential of the fractions and re-fractions of the stem extracts of *M. buxifolia*, TAC-, TRP-, and DPPH-based free-radical scavenging activities were performed. One of the mandatory natural phenomena is oxidation within biological systems generating highly reactive peroxyl and hydroxyl radicals.[27]

For the *n*-hexane fraction of the stem, the highest TAC and DPPH scavenging capabilities were observed in H16, that is,, 29.2 ± 0.7 μg AAE/mg extract and 45.0 ± 1.8%, respectively, while the highest TRP was observed in the H11 fraction (Figure 5A). Later, the column plotted for H9−H10, the highest TAC, and radical scavenging capability (DPPH) was observed in the 3rd fraction among the eight fractions (1−8), while the highest TRP was observed in the 8th fraction (Figure 5B).

The maximum TAC, TRP, and radical scavenging capability for the chloroform fraction ($CHCl_3$) were observed in the C9 fraction to be 35.2 ± 1.4 μg AAE/mg extract, 90.9 ± 1.4 μg

https://doi.org/10.1021/acsomega.1c05647
ACS Omega 2022, 7, 3407−3423

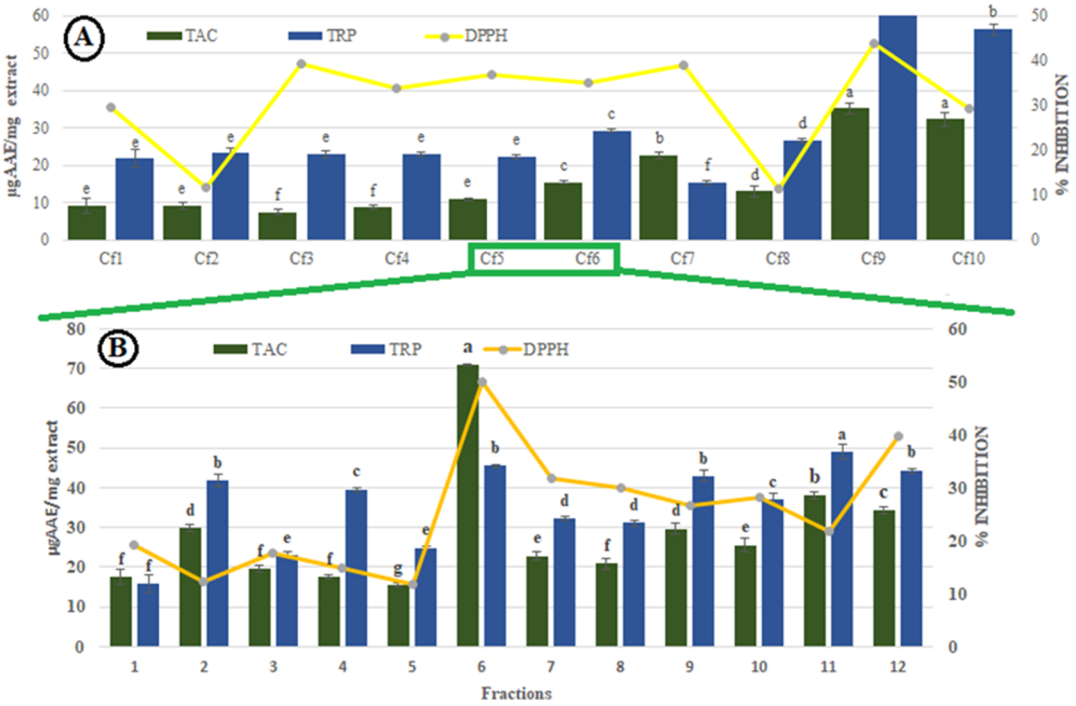

Figure 6. TAC, TRP, and DPPH of the $CHCl_3$ fractions of *M. buxifolia* stem. (A) TAC, TRP, and DPPH of C1−C10 fractions. (B) TAC, TRP, and DPPH of 1−12 subfractions of C5−C6 fractions.

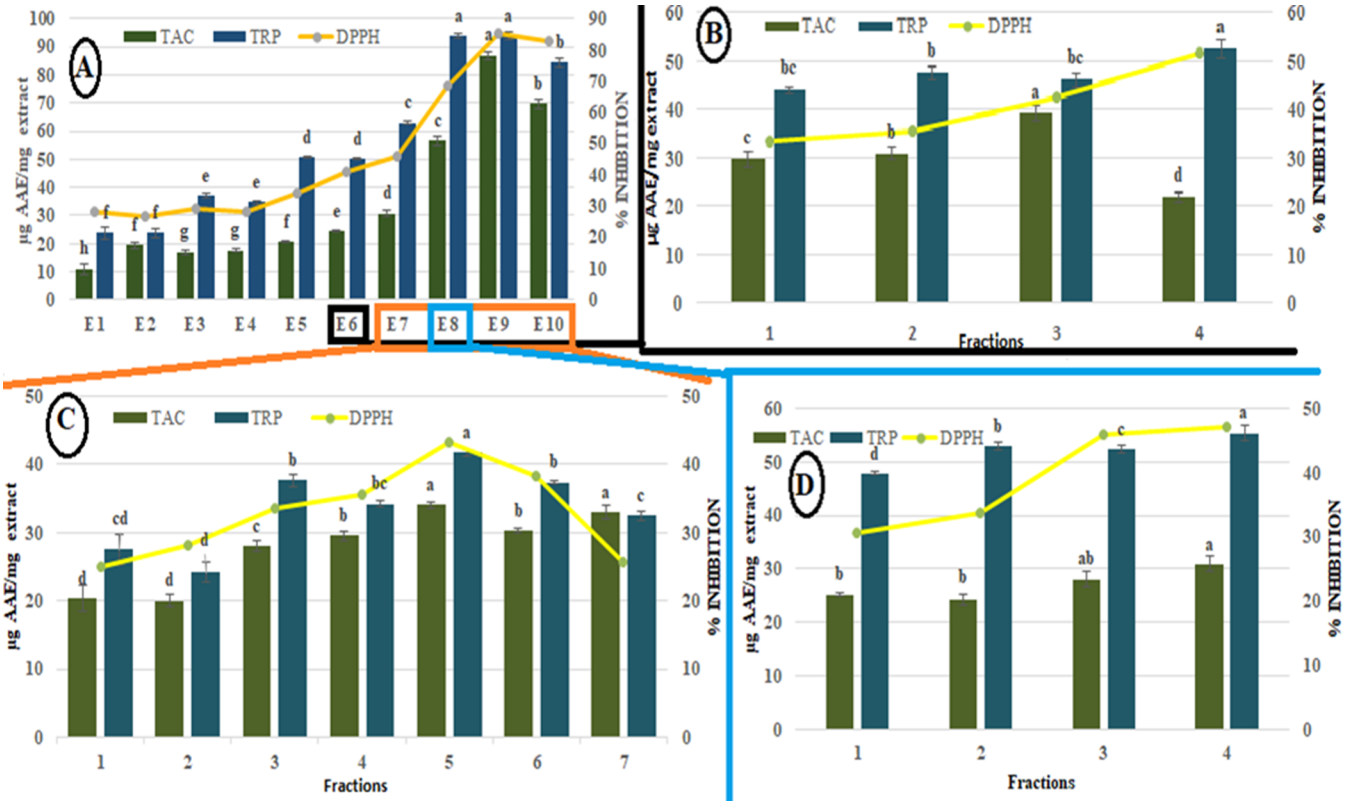

Figure 7. TAC, TRP, and DPPH of EtOAc fractions of *M. buxifolia* stem: (A) TAC, TRP, and DPPH of E1−E10 fractions; (B) TAC, TRP, and DPPH of 1−4 subfractions of E6 fraction; (C) TAC, TRP, and DPPH of 1−7 subfractions of E7, E9, and E10 (in combination) fractions; (D) TAC, TRP, and DPPH of 1−4 subfractions of E8 of EtOAc fractions.

AAE/mg extract, and 43.8 ± 1.4%, respectively (Figure 6A). The combination of C5−C6 fractions resulted in further 12 fractions, among which the highest antioxidant capacity in terms of TAC (70.9 ± 0.3 μg AAE/mg extract) and DPPH assays (50.1 ± 1.5%) was observed in the 6th fraction, while the highest reducing capability (49.0 ± 1.9 μg AAE/mg extract) was observed in the 11th fraction (Figure 6B).

https://doi.org/10.1021/acsomega.1c05647
ACS Omega 2022, 7, 3407−3423

Table 2. Biological Activities of the *n*-Hexane Fraction[a]

		protein kinase		brine shrimp	antibacterial zone (mm)					antifungal zone (mm)				
	amylase inhibition (%)	bald	clear	LD_{50}	*E. coli*	*P. aeruginosa*	*K. pneumoniae*	*B. species*	*S. aureus*	*A. flavus*	*A. fumigatus*	*A. niger*	*Mucor* sp	*F. solani*
Activity Response of *n*-Hexane Fractions														
H1	23.3	13 ± 0.9		24.9	11 ± 0.9	8 ± 0.8	7 ± 0.9	7 ± 0.9	7 ± 0.9		7 ± 0.8			
H2	12.3	13 ± 0.8		49.9	11 ± 0.8	9 ± 0.8	7 ± 0.8	7 ± 0.9	7 ± 0.8					
H3	19.7		20 ± 1.0	39.8	10 ± 0.7	8 ± 0.8	8 ± 0.7	8 ± 0.8	7 ± 0.7					
H4	20.6	13 ± 0.8		30.5	10 ± 0.7	7 ± 0.7	9 ± 0.6	7 ± 0.6	7 ± 0.6					
H5	19.0	11 ± 0.7		49.9	9 ± 0.7	8 ± 0.7	8 ± 0.5	8 ± 0.7	7 ± 0.5					
H6	18.1	14 ± 0.7	11 ± 0.8	99.9	8 ± 0.9	9 ± 0.9	7 ± 0.9	7 ± 0.8	9 ± 0.7					
H7	19.1	12 ± 0.7		24.8	7 ± 0.8	10 ± 1.0	8 ± 0.8	8 ± 0.7	7 ± 0.5					
H8	27.1	12 ± 0.9		24.8	7 ± 0.8	10 ± 1.0	8 ± 0.9	7 ± 1.0	13 ± 0.8					
H9	44.6	12 ± 0.8		199.8	15 ± 0.5	11 ± 0.9	9 ± 0.6	9 ± 1.0	11 ± 0.7		7 ± 0.8			
H10	33.4	12 ± 0.9		198.9	20 ± 1.0	12 ± 0.5	10 ± 0.8	15 ± 0.9	15 ± 0.8	9 ± 0.9	9 ± 0.7			9 ± 0.9
H11	37.3		11 ± 0.9	199.1	15 ± 0.9	12 ± 0.6	9 ± 0.7	10 ± 0.9	12 ± 0.9	10 ± 0.7	12 ± 0.5	12 ± 0.9		16 ± 0.8
H12	25.6		11 ± 0.9	197.9	15 ± 0.8	9 ± 1.0	8 ± 0.9	16 ± 1.0	8 ± 0.8	11 ± 0.8	12 ± 0.6	9 ± 0.8		16 ± 0.7
H13	25.5		11 ± 0.9	190.2	9 ± 0.7	9 ± 0.9	10 ± 0.9	16 ± 1.0	18 ± 0.7	11 ± 0.8	14 ± 0.6	13 ± 0.9		16 ± 0.7
H14	15.8		10 ± 0.8	186.7	10 ± 0.9	8 ± 0.9	9 ± 1.0	10 ± 0.8	12 ± 1.0			7 ± 0.6		
H15	15.5		12 ± 0.9	168.9	8 ± 0.9	9 ± 0.8	7 ± 0.9	7 ± 0.8	7 ± 1.1			7 ± 0.6		
H16	16.8		12 ± 1.0	187.9	22 ± 1.0	13 ± 0.8	9 ± 0.8	7 ± 0.8	7 ± 0.9			7 ± 0.5		
Activity Response of Fractions 1−8 of H9−H10														
1	36.8	9 ± 0.9		38.7	8 ± 0.9		9 ± 0.9	10 ± 0.9		9 ± 0.9		7 ± 0.9	8 ± 0.7	
2	25.3	9 ± 0.8		24.9		8 ± 0.9	9 ± 1.0	10 ± 0.8	9 ± 0.9			8 ± 0.8	8 ± 0.6	
3	34.5	10 ± 0.9		24.1	8 ± 0.8	7 ± 0.8			9 ± 0.8	8 ± 0.8	10 ± 0.9	9 ± 0.7		9 ± 0.6
4	25.9	8 ± 1.0	11 ± 0.9	24.8	8 ± 0.8	7 ± 0.7			7 ± 0.5	8 ± 0.7	11 ± 0.8	10 ± 0.9	10 ± 0.5	
5	32.0		11 ± 0.8	24.9	8 ± 0.7	9 ± 0.0		9 ± 0.7	9 ± 0.4	8 ± 0.3	10 ± 0.7			8 ± 0.7
6	31.4	10 ± 0.7		24.2			10 ± 0.9		8 ± 0.3		10 ± 0.6		11 ± 0.4	
7	32.6	9 ± 0.6		24.8			11 ± 0.8	7 ± 1.0					10 ± 0.8	
8	27.7	8 ± 0.9		49.9	10 ± 1.0	12 ± 1.0	13 ± 0.7	7 ± 1.1		9 ± 0.7		10 ± 1.0		10 ± 0.9
Standards														
Rox					26 ± 0.8	19 ± 0.8	25 ± 1.0	23 ± 1.0	20 ± 1.0					
Surfac		17 ± 1.2												
Dox				23.93										
Clotrim										24 ± 1.0	22 ± 0.4	25 ± 0.6	22 ± 1.1	23 ± 0.8
DMSO														

[a](H1−H16) fractions were collected from the fractionation of the *n*-hexane fraction of stems using CC.

https://doi.org/10.1021/acsomega.1c05647
ACS Omega 2022, 7, 3407−3423

Table 3. Biological Activities of $CHCl_3$ Fractions[a]

		protein kinase		brine shrimp	antibacterial zone (mm)					antifungal zone (mm)				
	amylase inhibition (%)	bald	clear	LD_{50}	*E. coli*	*P. aeruginosa*	*K. pneumoniae*	*B. species*	*S. aureus*	*A. flavus*	*A. fumigatus*	*A. niger*	*Mucor* sp	*F. solani*
Activities of $CHCl_3$ Extract Fractions														
C1	13.5	11 ± 1.1		24.5	7 ± 1.1	7 ± 0.9	9 ± 0.6	9 ± 0.8	11 ± 0.9	10 ± 1.0		8 ± 0.9		
C2	14.2			98.7	7 ± 0.9	8 ± 0.8	8 ± 0.5	7 ± 0.6	7 ± 0.7		7 ± 1.0	9 ± 0.8	10 ± 0.9	7 ± 1.1
C3	11.8		13 ± 0.9	40.3		7 ± 1.2	7 ± 0.4	7 ± 0.8	9 ± 0.6	10 ± 0.6	8 ± 0.9	9 ± 0.8	9 ± 0.8	
C4	15.7		14 ± 0.8	49.3	8 ± 0.7	7 ± 0.8	7 ± 0.7	7 ± 0.9	8 ± 1.1	6 ± 0.9	9 ± 0.7	9 ± 1.3	10 ± 0.7	9 ± 0.9
C5	28.9		12 ± 0.7	24.1	7 ± 0.5	8 ± 0.7	7 ± 0.3		12 ± 1.2	7 ± 0.8	11 ± 0.5		9 ± 0.7	8 ± 1.2
C6	29.9		12 ± 0.9	22.3	8 ± 0.6	10 ± 0.6	8 ± 1.1	8 ± 0.5	9 ± 0.8	9 ± 0.8	8 ± 0.4		9 ± 0.8	
C7	19.9		16 ± 1.0	49.8	8 ± 0.3	9 ± 0.6		7 ± 0.9	10 ± 0.6		8 ± 0.9	10 ± 1.0	8 ± 0.9	10 ± 0.8
C8	8.8		13 ± 1.1	35.4	7 ± 1.5	7 ± 0.4	9 ± 1.2	7 ± 0.3	12 ± 0.7	11 ± 0.9	9 ± 0.8	8 ± 1.1	9 ± 1.0	
C9	43.0		11 ± 1.0	49.7	7 ± 1.2	8 ± 0.9	9 ± 1.3	10 ± 0.9	9 ± 1.0	9 ± 0.7		8 ± 0.9	10 ± 1.2	11 ± 0.7
C10	17.2		9 ± 0.9	24.3	8 ± 1.0			9 ± 1.1	11 ± 1.0	8 ± 0.6	10 ± 0.7	8 ± 0.8		
Activity Response of Fractions 1−12 of C5−C6														
1	26.8		9 ± 0.6	24.13			10 ± 1.3		7 ± 0.9	9 ± 0.6			10 ± 0.9	
2	32.0		8 ± 0.5	24.12	8 ± 1.1	9 ± 0.9				8 ± 0.5		8 ± 0.6	9 ± 0.7	8 ± 0.9
3	39.1	14 ± 1.1		23.18			8 ± 1.5	9 ± 0.6		8 ± 1.4	8 ± 0.8	7 ± 0.9	8 ± 0.5	9 ± 0.8
4	25.3		7 ± 0.7	49.19	10 ± 1.4	7 ± 0.6				8 ± 1.5	8 ± 0.9		8 ± 1.2	10 ± 1.1
5	73.3	13 ± 1.1		198.4			11 ± 1.5	8 ± 0.9	8 ± 0.6	7 ± 0.9	8 ± 1.1	7 ± 1.1	8 ± 1.3	
6	48.8		9 ± 0.5	199.89		10 ± 0.7					10 ± 1.6		7 ± 1.6	7 ± 1.2
7	90.4		7 ± 0.4	45.7			9 ± 1.3	9 ± 0.8		10 ± 0.6		12 ± 1.2		7 ± 1.3
8	41.9		10 ± 0.8	22.89	11 ± 0.9		10 ± 0.9		10 ± 1.3	10 ± 1.3	10 ± 1.1			8 ± 0.9
9	18.0		8 ± 0.9	49.97		9 ± 0.9		10 ± 1.2		10 ± 0.8	12 ± 0.8		10 ± 0.9	9 ± 0.8
10	23.7		8 ± 1.1	24.61						8 ± 1.4		10 ± 0.9	10 ± 0.7	10 ± 0.7
11	16.8		7 ± 0.9	24.55	9 ± 0.7	12 ± 0.6	10 ± 1.2	10 ± 1.4	12 ± 0.9		12 ± 0.6	9 ± 0.7	10 ± 0.5	10 ± 0.6
12	17.8	12 ± 0.9		49.88	9 ± 1.1	16 ± 1.1		20 ± 1.2	15 ± 1.1			8 ± 0.9	9 ± 0.8	10 ± 1.1
Standards														
Rox					26 ± 0.8	19 ± 0.8	25 ± 1.0	23 ± 1.0	20 ± 1.0					
Surfac		17 ± 1.2												
Dox				23.93										
Clotrim										24 ± 1.0	22 ± 0.4	25 ± 0.6	22 ± 1.1	23 ± 0.8
DMSO														

[a]C1−C10 are fractions collected from the fractionation of the $CHCl_3$ fraction of stems using CC.

https://doi.org/10.1021/acsomega.1c05647
ACS Omega 2022, 7, 3407−3423

Table 4. Biological Activities of EtOAc Fractions[a]

		protein kinase		brine shrimp	antibacterial zone (mm)					antifungal zone (mm)				
	amylase inhibition (%)	bald zone	clear zone	LD_{50}	*E. coli*	*P. aeruginosa*	*K. pneumoniae*	*B. species*	*S. aureus*	*A. flavus*	*A. fumigatus*	*A. niger*	*Mucor* sp	*F. solani*
Activity Response of EtOAc Fractions														
E1	32.5		24 ± 0.9	188		15 ± 0.7	13 ± 0.9		13 ± 1.1					
E2	27.3		20 ± 0.5	45.6				13 ± 0.9	13 ± 0.9				12 ± 0.8	
E3	17.1		22 ± 0.8	24.8	15 ± 0.9				13 ± 0.8					
E4	25.7		22 ± 0.9	86.7					13 ± 0.8				14 ± 0.9	
E5	23.8		25 ± 1.0	24.3	16 ± 1.0	16 ± 0.6	15 ± 0.8	15 ± 0.8	15 ± 0.7	13 ± 0.8		15 ± 0.7	20 ± 0.7	14 ± 1.2
E6	44.9		22 ± 0.6	178.6	17 ± 1.2		15 ± 1.0	14 ± 1.3	17 ± 1.0				18 ± 0.6	
E7	22.3		25 ± 0.5	187.9	12 ± 0.9		20 ± 1.2		15 ± 1.2					
E8	50.7		22 ± 0.9	189.7		16 ± 1.2	14 ± 1.3		15 ± 1.3					
E9	52.6		27 ± 1.0	189.6	15 ± 0.8	15 ± 1.3			15 ± 1.2	14 ± 0.9				
E10	54.3		20 ± 1.1	177.8		16 ± 0.9			15 ± 1.1					
Activity Response of Fractions 1−4 of E6														
1	36.7			24.9	16 ± 0.8			18 ± 0.6	15 ± 0.6			9 ± 0.5		9 ± 0.7
2	36.8			26.8				20 ± 0.5		10 ± 0.9		9 ± 0.8	8 ± 0.7	
3	28.0		23 ± 0.9	24.9	15 ± 0.9			17 ± 1.0				11 ± 0.6	8 ± 0.5	
4	33.6			27.8				20 ± 0.9	16 ± 0.9			8 ± 1.2	8 ± 0.9	10 ± 0.5
Activity Response of Fractions 1−7 of E7−E10 (Excluding E8)														
1	36.2		33 ± 0.5	24.9	17 ± 0.6	15 ± 0.6			16 ± 0.7	9 ± 0.9		8 ± 0.6		10 ± 0.6
2	38.2		33 ± 0.6	35.7		21 ± 0.5				9 ± 0.8		8 ± 0.5	10 ± 0.9	9 ± 1.0
3	35.8		17 ± 0.4	98.8		19 ± 1.0			21 ± 0.5		11 ± 0.6	7 ± 0.4	9 ± 0.5	10 ± 0.6
4	37.5		24 ± 0.9	199.8	20 ± 0.9	19 ± 0.9			20 ± 0.7		9 ± 0.6		9 ± 0.8	11 ± 0.5
5	41.4		20 ± 0.8	197.5		20 ± 0.5				10 ± 1.0	9 ± 0.5		8 ± 0.7	
6	32.4		21 ± 0.9	87.9		20 ± 0.9				11 ± 0.7		11 ± 1.0	10 ± 0.4	
7	28.3			67.8							10 ± 0.4	11 ± 0.9		12 ± 0.6
Activity Response of Fractions 1−4 of E8														
1	29.7		28 ± 0.7	26.5										
2	27.3		28 ± 1.0	87.6			16 ± 0.8	18 ± 0.8	24 ± 1.0			11 ± 0.7		
3	35.8		32 ± 0.9	88.7	15 ± 0.5	14 ± 0.6	15 ± 0.6	18 ± 0.5	24 ± 0.9		12 ± 0.6			19 ± 0.9
4	35.7		28 ± 0.5	24.9	15 ± 0.6	15 ± 0.9					12 ± 0.5	12 ± 0.8	12 ± 0.9	19 ± 0.5
Standards														
Rox					26 ± 0.8	19 ± 0.8	25 ± 1.0	23 ± 1.0	20 ± 1.0					
Surfac		17 ± 1.2												
Dox				23.93										
Clotrim										24 ± 1.0	22 ± 0.4	25 ± 0.6	22 ± 1.1	23 ± 0.8
DMSO														

[a]E1−E10 are fractions collected from the fractionation of the EtOAc fraction of stems through CC.

https://doi.org/10.1021/acsomega.1c05647
ACS Omega 2022, 7, 3407−3423

For the EtOAc fraction, the highest TRP and DPPH activities were observed in E9, that is, 94.0 ± 1.4 μg AAE/mg extract and 85.2 ± 1.5%, while the highest TAC was observed in E10, that is, 69.7 ± 1.7 μg AAE/mg extract (Figure 7A). Among the subfractions of E6, the 4th fraction showed the maximum TRP and DPPH activity, that is, 52.5 ± 1.9 μg AAE/mg extract and 51.6 ± 0.3%, respectively, while the highest TAC was observed in the third fraction, that is, 39.3 ± 1.7 μg AAE/mg extract (Figure 7B). Among the subfractions (1−7) of E7, E9, and E10 (in combination), the 5th fraction depicted the maximum TAC (34.0 ± 0.4 μg AAE/mg extract), TRP (41.7 ± 0.4 μg AAE/mg extract), and DPPH (43.3 ± 0.4%) activities (Figure 7C). For E8 fraction's subfractions, the 4th fraction showed the highest TAC, TRP, and DPPH activities (30.9 ± 1.4 μg AAE/mg extract, 55.4 ± 1.4 μg AAE/mg extract, and 47.1 ± 0.5%, respectively) (Figure 7D). Positive correlation was observed between the reducing power and the antioxidant potential of all the test samples and to that of phenolic and flavonoid contents.

α-Amylase Inhibition Assay. The prevailing *Diabetes mellitus* patients worldwide and in developing countries demand the identification of inhibitors of α-glucosidase and α-amylase (carbohydrates digesting enzymes).[28,29] H9 from the *n*-hexane fraction showed the highest inhibition of 44.6%, while among the fractions of H9−H10, the first fraction depicted the highest α-amylase inhibition (Table 2).

Among $CHCl_3$ fractions, C6 showed 29.9% inhibition, while among the C5−C6 column re-fractions, the 7th fraction presented the highest percent inhibition, that is, 90.4% (Table 3). Among the fractions of the EtOAc extract, E10, E9, E8, and E6 displayed good inhibition tendency sequentially, that is, 54.3, 52.6, 50.7, and 44.9%, respectively (Table 4). Though the fractionation of E6 and E8 did not show any promising activity, the fractionation of E7, E9, and E10 (in combination), in comparison to these two, was still diagnosed with good amylase inhibition activity. Its 5th fraction displayed 41.4% inhibition (Table 4).

Protein Kinase Inhibition Assay. Protein kinase inhibition is a remarkable assay for cancer treatment. The cancer-induced property is associated with phosphorylation at serine/threonine and tyrosine residues during the initial stage of tumorigenesis.[30] *Streptomyces 85E* is used as the kinase inhibition strain that helps in marking a variety of eukaryotic kinase modulators as the enzymes of *Streptomyces* are the forerunners of highly specific eukaryotic counterparts. The fractions and re-fractions involved in this study showed clear zones except for few (Tables 2−4). Bald zone is more significant for this assay as it indicates the hyphae inhibition leading to its preliminary anticancer potential. The fractionation of the *n*-hexane extract H6 showed a significant bald ZOI of 14 mm while a clear ZOI of 20 mm by H3 (Table 2). The $CHCl_3$ fraction did not show cytotoxicity against *Streptomyces* as no clear zone and no obvious bald ZOI were observed, except for the 3rd, 5th, and 12th fractions of the C5−C6 column (Table 3). The EtOAc fractions and re-fractions depicted significant clear zones, but no bald zone was observed (Table 4). The results suggest that the tested samples (fractions and re-fractions) can be processed for the isolation of active constituents against the *Streptomyces* strain. A key feature of this assay is that it is precisely helpful in the identification of signal transduction inhibitors for antitumor and anti-infective entities.[31]

Brine Shrimp Lethality Assay. *Artemia salina* (brine shrimp) larvae were used to evaluate the cytotoxic potential of the fractions and re-fractions of the stems of *M. buxifolia*. All fractions (*n*-hexane, $CHCl_3$, and EtAOc) and re-fractions depicted toxic effects (LC_{50} values < 1000 μg/mL) that confirmed the presence of components responsible for the toxicological activity, ranging from 22 to 200 μg/mL (Tables 2−4). All fractions and re-fractions tended to be outstanding, but C6 of $CHCl_3$ depicted the lowest LC_{50} of 22.3 μg/mL, even lesser than that of the standard drug used. This cytotoxicity test was performed to identify the safety and ethnopharmacological importance of fractions and re-fractions.[32] Further investigation using *in vitro* cancer cell lines is recommended in regard to the plant's cytotoxic potential.

Antibacterial Assay. Antibacterial activity relies on different plant parts, extraction methodology, type of solvent, and microorganisms under scrutiny.[33] For the *n*-hexane fraction, the highest ZOI was observed for H11 and H12 against *Bacillus species,* that is, 16 mm, while H12 was found to be active against *Staphylococcus aureus* (18 mm ZOI). On the other hand, fraction H16 gave significant ZOI against *Escherichia coli* and *P. aeruginosa* (22 and 13 mm, respectively), as shown in Table 2.

The highest ZOI for the chloroform fractions of stems was depicted in C5 and C8 (12 mm each) against *S. aureus* (Table 3). For the chloroform re-fractions obtained from C5−C6, the highest activity was observed in the 12th fraction against *Bacillus species*, *P. aeruginosa,* and *S. aureus* (20, 16, and 15 mm, respectively), as shown in Table 3.

For ethyl acetate fractions, ample number of fractions tended to be active against the bacterial strains (Table 4), among which E5 ought to be active against *P. aeruginosa* (16 mm ZOI) and *Bacillus species* (15 mm ZOI). E6 was found potent against *E. coli* and *S. aureus* strains (17 mm each), while E7 was active against *K. pneumoniae* and *P. aeruginosa* (20 and 16 mm, respectively). Ethyl acetate re-fractions separated from the E6 column (1st, 2nd, and 4th fractions) tended to be active against *E. coli*, *Bacillus species,* and *S. aureus* (Table 4). The re-fractions separated from columns E7, E9, and E10 (in combination) resulted in seven fractions, among which the highest activity was observed in the 2nd fraction against *P. aeruginosa* and 4th fraction against *E. coli* and *S. aureus* (21, 20, and 20 mm, respectively). Among the re-fractions of the E8 column, the highest ZOI was observed against *K. pneumoniae*, *Bacillus species,* and *S. aureus* by the 2nd fraction (16, 18, and 24 mm, respectively), while the highest activity against *E. coli* and *P. aeruginosa* was observed by the 4th fraction (15 mm each), as shown in Table 4. Phenolic (hydroxylated) compounds like caffeic acid and catechol retrieved from various plant extracts are known to be lethal against microorganisms.[34]

Antifungal Assay. Plant-derived secondary metabolites (phenols, phenolic glycosides, flavonoids saponins, sulfur-based compounds, cyanogenic glycosides, and glucosinolates) are well-known antifungal agents.[35] Among the *n*-hexane fractions, the highest ZOI was observed for H13 against *A. fumigatus*, *A. niger,* and F. *solani* (14, 13, and 16 mm, respectively) (Table 2). No significant results were obtained when the re-fractions of *n*-hexane (H9−H10) were tested against the fungal strains. No significant ZOI was observed for the $CHCl_3$ fractions and re-fractions (Table 3).

For ethyl acetate fractions, the highest antifungal capacity was observed in E5 against *A. niger*, *Mucor species,* and F. *solani* (15, 20, and 14 mm, respectively), while E9 presented significant activity against *A. flavus* (14 mm). Ethyl acetate re-fractions obtained from CC did not show any significant activity against the fungal strains except few (Table 4).

https://doi.org/10.1021/acsomega.1c05647
ACS Omega 2022, 7, 3407−3423

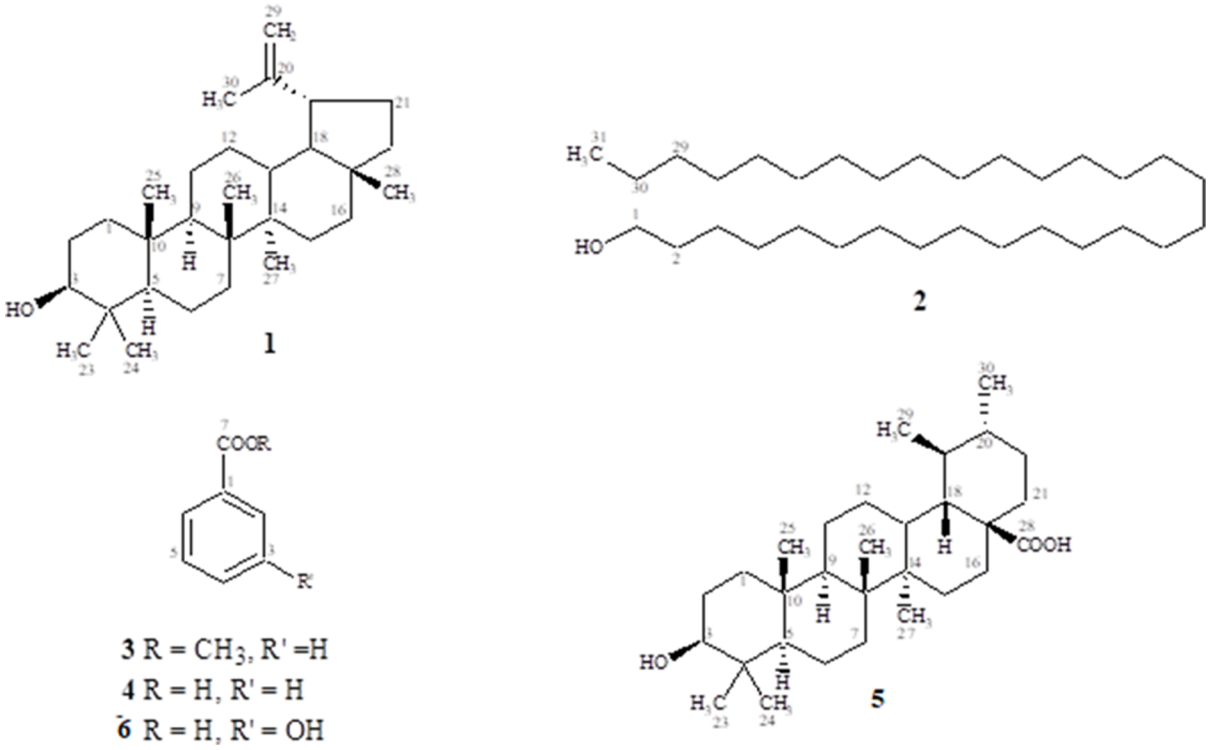

Figure 8. Structure of compounds isolated from *M. buxifolia* through bioguided isolation. Compound **1** (lupeol); compound **2** (1-triacontanol); compound **3** (methyl benzoate); compound **4** (benzoic acid); compound **5** (ursolic acid); and compound **6** (3-hydroxybenzoic acid).

Structure Elucidation of Compounds. *Compound 1 (Lupeol Am-6, AM-7, AM-8).* Compound **1** (Lupeol Am-6, AM-7, AM-8) was isolated as a colorless amorphous powder. Its IR spectrum showed the absorption bands at 3400, 2920, and 1640 cm^{-1}, indicating the presence of O−H, C−H, and C═C functionalities. The ^{1}H NMR spectrum showed the presence of seven tertiary methyl groups at δ 1.70, 1.05, 1.00, 0.97, 0.85, 0.81, and 0.78 (3H each, s). It also showed two singlets at δ 4.70 and 4.59 (1H each, s) and an oxymethine group at δ 3.20 (1H, dd, J = 11.2, 5.0 Hz, H-3). The ^{13}C NMR spectra (BB & DEPT) of **1** showed altogether 30 carbon signals which revealed the presence of seven methyl, eleven methylene, six methine, and six quaternary carbons. The downfield shifts that appeared at δ 151.01, 109.33, and 79.03 were assigned to the olefin and aliphatic oxymethine carbons, respectively. The signals for the seven tertiary methyls appeared at δ 28.00, 19.31, 18.01, 16.13, 15.98, 15.38, and 14.56. The molecular formula $C_{30}H_{50}O$ was deduced from the data of high-resolution electron ionization mass spectrometry (HREIMS), which showed the molecular ion peak at m/z 426.3880 with six double-bond equivalences. Its EIMS spectrum showed the major fragments at m/z 4.11, 315, 218, 207, 203, 189, 147, 135, and 95. By the evaluation of the above data and by searching in the literature, it was observed that the discussed data fully overlapped with the data already reported for lup-20(29)-en-3β-ol (lupeol).[36]

Compound 2 (1-Triacontanol Am-2). Compound **2** (1-triacontanol Am-2) was isolated as a white amorphous powder. Its IR spectrum showed peaks at 3395 and 2955, attributed to the O−H and C−H functionalities. The ^{1}H NMR spectrum showed that a triplet at δ 3.62 (2H, t, J = 6.8 Hz), a multiplet at 1.52 (2H, m), a broad singlet at 1.23 (54H, br s), and a triplet at 0.86 (3H, t, J = 6.8 Hz) resulted for a typical aliphatic alcohol. Its ^{13}C NMR spectra (BB & DEPT) supported the ^{1}H NMR spectrum, as it showed the presence of a primary alcohol at δ 63.1, an aliphatic chain due to signals at δ 32.8−29.4, 25.8, and 22.7, and a terminal methyl at δ 14.1. The molecular formula $C_{30}H_{62}O$ was confirmed by HREIMS that showed the molecular ion peak at m/z 438.44820. The EIMS spectrum showed the major fragments m/z 395, 381, 367, and 325 and the base peak at 120. Based on the above discussion, the compound is confirmed as 1-triacontanol (Figure 8).

Compound 3 (Methyl Benzoate EM-6). Methyl benzoate was isolated as a colorless liquid. Its IR spectrum showed the absorption bands at 1755 (C═O), 1620−1499 (Ar C═C), and 1165 (C−O). The aromatic region of the ^{1}H NMR spectrum displayed the same signals at δ 8.10 (2H, d, J = 8.5 Hz, H-2,6), 7.61 (1H, t, J = 8.5 Hz, H-4), and 7.45 (2H, t, J = 8.5 Hz, H-3,5). The missing broad signal in the downfield region with the appearance of methyl at δ 3.80 (3H, s) clued us about the protection of acid with the methyl group. The ^{13}C NMR (BB & DEPT) spectrum disclosed, altogether, six carbon signals for eight carbons including a methyl, three methine, and two quaternary carbon atoms. The downfield signal that resonated at δ 168.3 was assigned to ester carbonyl, whereas the remaining signals in the aromatic region at δ 135.4, 130.6, 129.9, and 131.7 were assigned to aromatic methines and aromatic quaternary carbon atoms. HREIMS showed a molecular ion peak at m/z 136.0544 corresponding to the molecular formula $C_8H_8O_2$ (calcd for $C_8H_8O_2$, 136.0524). The above spectral data were found to completely overlap with the data reported for methyl benzoate (Figure 8).

Compound 4 (Benzoic Acid EM-11). Compound **4** (benzoic acid EM-11) was isolated as colorless needles. The IR spectrum showed the absorption bands at 3260−2612 (COOH), 1696 (C═O), and 1626−1494 (Ar C═C). The ^{1}H NMR spectrum displayed three signals in the aromatic region at δ 8.12 (2H, d, J = 8.5 Hz, H-2,6), 7.60 (1H, t, J = 8.5 Hz, H-4), and 7.46 (2H, t, J = 8.5 Hz, H-3,5), together with a broad signal in the most

https://doi.org/10.1021/acsomega.1c05647
ACS Omega 2022, 7, 3407−3423

Table 5. Biological Activities of Compounds Isolated from *M. buxifolia* Stem Extracts

	compound **1**	compound **2**	compound **3**	compound **4**	compound **5**	compound **6**
compound	lupeol	1-triacontanol	benzaldehyde benzoate	benzoic acid	ursolic acid	3-hydroxybenzoic acid
			Phytochemical and Antioxidant Analyses			
TAC μgAAE/mg extract	55.5 ± 1.3	89.5 ± 1.6	82.5 ± 1.3	60.6 ± 1.8	70.4 ± 1.8	66.6 ± 1.5
TRP μgAAE/mg extract	96.9 ± 1.6	55.2 ± 1.8	45.2 ± 1.6	59.5 ± 1.5	76.2 ± 1.5	62.5 ± 1.3
DPPH %	68.8 ± 1.1	59.4 ± 2.1	49.4 ± 1.9	50.8 ± 1.6	58.6 ± 1.7	65.8 ± 1.6
			Enzyme Inhibition %			
amylase	16.0 ± 0.4	29.9 ± 1.4	26.2 ± 0.5	36.5 ± 0.9	48.9 ± 0.6	31.5 ± 0.8
urease	85.8 ± 0.9	82.5 ± 0.8	55.1 ± 1.2	65.8 ± 0.6	78.8 ± 0.5	59.8 ± 0.6
lipase	84.0 ± 0.8	50.8 ± 0.9	50.3 ± 0.5	58.9 ± 0.7	76.6 ± 0.8	51.9 ± 0.7
			Antibacterial (mm)[a]			
M. luteus	15 ± 1.1	10 ± 0.9	14 ± 1.1	13 ± 1.2	14 ± 1.4	15 ± 1.2
S. aureus	14 ± 1.2	9 ± 1.3	7 ± 0.8	12 ± 1.6	13 ± 1.3	15 ± 1.6
S. typhi	18 ± 1.3	10 ± 1.3	10 ± 1.1	15 ± 1.5	16 ± 1.8	16 ± 1.5
E. aerogenes	14 ± 1.1	15 ± 1.4	15 ± 1.1	12 ± 1.4	12 ± 1.3	15 ± 1.4
S. setubal	12 ± 1.3	15 ± 1.2	13 ± 1.1	15 ± 1.7	13 ± 1.2	14 ± 1.7

[a]Cefixime was used as a positive control in the antibacterial assay that showed ZOI of 20.5 ± 1.4 mm against *M. luteus*; 23.5 ± 1.6 mm against *S. aureus*; 22.5 ± 1.1 mm against *S. typhi*; 26 ± 1.8 mm against *E. aerogenes*; and 20 ± 1.2 mm against *S. setubal*.

downfield region for carboxylic acid at δ 11.92 (1H, br s). The ^{13}C NMR (BB & DEPT) spectrum disclosed five carbon signals in total for seven carbons, including three methine and two quaternary carbon atoms. The downfield signal that resonates at δ 173.0 was assigned to acid carbonyl, whereas the remaining signals in the aromatic region at δ 134.5, 130.7, 129.7, and 131.4 were assigned to aromatic methines and aromatic quaternary carbon atoms. HREIMS showed a molecular ion peak at m/z 122.0387 corresponding to the molecular formula $C_7H_6O_2$ (calcd for $C_7H_6O_2$, 122.0367). The above spectral data showed complete resemblance with the data reported for benzoic acid (Figure 8).

Compound ***5*** *(Ursolic Acid EM-9).* It was purified as a colorless amorphous solid, which showed a pink spot on TLC when located with ceric sulfate on heating. The IR spectrum disclosed bands at 3435, 3019, 2927, and 1643 cm^{-1}, indicating the presence of alcoholic, saturated, and unsaturated functionalities. The ^{1}H NMR spectrum of **2** exhibited signals for an olefinic proton at δ 5.23 (1H, t, J = 5.6 Hz), an oxymethine at δ 3.25 (1H, dd, J = 11.5, 5.2 Hz), and seven methyls at δ 1.19, 0.97, 0.93, 0.89, 0.76 (3H each, s), and 0.87, 0.84 (3H each, d, J = 7.1 Hz), characteristic for an ursane skeleton. The ^{13}C NMR spectra (BB and DEPT) of **2** showed, altogether, 30 carbon signals for seven methyl, nine methylene, seven methine, and seven quaternary carbons. The downfield signals at δ 179.6, 138.9, 125.1, and 78.8 were assigned to carboxylic acid, olefin, and aliphatic oxygenated methine carbons. Its molecular formula was established from the data of HREIMS, which showed the molecular ion peak at m/z 456.3620, indicating the presence of seven degrees of unsaturation. Its EIMS spectrum showed the fragments at m/z 248 along with a strong peak at m/z 203 due to retro-Diels−Alder fragmentation, typical of Δ^{12}-ursine triterpene with the molecular formula $C_{30}H_{48}O_3$.[37] The whole characterization was completed by comparison with the reported data for 3β-hydroxy-urs-12-en-28-oic acid [ursolic acid (Figure 8)].[38]

Compound ***6*** *(3-Hydroxybenzoic Acid EM-7).* 3-Hydroxybenzoic acid was purified as a colorless crystalline solid. The IR spectrum showed the absorption bands at 3255−2615 (COOH), 1692 (C═O), 1626−1494 (Ar C═C), and 1165 (C−O). The ^{1}H NMR spectrum displayed three signals in the aromatic region at δ 7.43 (1H, s, H-2), 7.36 (1H, d, J = 8.5 Hz, H-6), 7.30 (1H, t, J = 8.5 Hz, H-5), and 7.02 (1H, t, J = 8.5 Hz, H-4). In addition, a broad signal was resonated at δ 11.85 (1H, br s) for carboxylic acid. The ^{13}C NMR (BB & DEPT) spectrum disclosed seven carbon signals in total for four methine and three quaternary carbon atoms. The downfield signal that resonated at δ 170.3 was assigned to acid carbonyl, whereas the signals for the aromatic region at δ 157.4, 132.1, 129.6, 120.1, and 115.9 were due to the aromatic methines and aromatic quaternary carbon atoms. The molecular formula $C_7H_6O_3$ deduced by HREIMS showed a molecular ion peak at m/z 138.0336. The above spectral data completely overlapped with the data reported for 3-hydroxybenzoic acid.[39]

Biological Activities of Isolated Compounds. The compounds isolated after fractionation and re-fractionation were also analyzed for biological activities. Among the antioxidative set of activities, lupeol showed 96.9 μg AAE/mg and 68.8% free-radical scavenging activity. The highest TAC activity was observed by 1-triacontanol (89.5 μg AAE/mg) and methyl benzoate (82.5 μg AAE/mg). 3-Hydroxybenzoic acid also depicted significant activities, with the highest free-radical scavenging activity of 65.8% and antibacterial activity. Ursolic acid also depicted significant activities. All the compounds showed significantly higher urease (55.1−85.8%) and lipase (50.3−84.0%) inhibition activities, while ursolic acid was significantly active against amylase (48.9% inhibition) (Table 5). Most of the compounds extracted from the stem extract of *M. buxifolia* exhibited good antibacterial activity. Lupeol, benzoic acid, 3-hydroxybenzoic acid, and ursolic acid presented ZOI >12 mm against the bacterial strains tested, with the maximum ZOI of 18 mm by lupeol and 15 and 16 mm by benzoic acid and ursolic acid, respectively, against *Salmonella typhi*. Average ZOI of 15 mm was also observed against *Escherichia aerogenes* and *S. setubal* by 1-triacontanol. Methyl benzoate also depicted significant activity against *M. luteus* and *E. aerogenes*. Lupeol possesses a range of biological activities including antibacterial,[40,41] antifungal,[40,42] anticancer,[22,43,44] anti-inflammatory, and so forth, and is also a potential candidate to be used as a food supplement to prevent diseases.

On the other hand, methyl benzoate and its derivatives have pesticidal and insecticidal effects and are therefore considered as green pesticides.[45,46] Ursolic acid is one of the major components of some traditional medicinal plants and possesses

https://doi.org/10.1021/acsomega.1c05647
ACS Omega 2022, 7, 3407−3423

a wide range of biological activities, such as antioxidative, anti-inflammatory, and anticancer activities, that are able to counteract endogenous and exogenous biological stimuli.[47,48]

CONCLUSIONS

There is scarce data on the detailed evaluation of plant extracts for compound isolation, using bioassay-guided isolation techniques. The work entailing a thorough study of different fractions and re-fractions of the stem extracts of *M. buxifolia,* screening their phytochemical and biological potential, suggests this plant part as a potent source of bioactive constituents. The plant is an ample source of antioxidant agents, enzyme inhibitors, protein kinase inhibitors, and antimicrobial agents. The fractionation process turned out to be effective as the biological potential of fractions increased after each fractionation due to purification. Significant antioxidant potential was observed in the EtOAc fraction, while *n*-hexane and $CHCl_3$ had marked cytotoxic potency. This study paves the way for future research in order to isolate the bioactive compounds contributing to the folkloric use of a particular medicinal plant in the treatment of various ailments. The isolated compounds could act as scaffolds in modern research for the identification and isolation of novel drugs. Bioassay-guided isolation using fractionation and re-fractionation is recommended.

MATERIALS AND METHODS

Collection of Plant Materials. Fresh stems of *M. buxifolia* (Falc.) A. DC. was collected from Mohmand Agency, Khyber Pakhtunkhwa (KPK), Pakistan, in June 2016. It was identified by Dr. Rizwana Aleem Qureshi, Plant Taxonomist, Department of Plant Sciences, Quaid-i-Azam University, Islamabad, Pakistan. Voucher specimen (specimen no. BIT-4220) was deposited in the Herbarium, Quaid-i-Azam University, Islamabad, Pakistan.

Extraction Procedure. The fresh stems were thoroughly washed with tap water to remove impurities and dust and shade-dried for 2 weeks. An electrical grinder was used to pulverize the dried stems into powder. Crude methanol extract was prepared by suspending the plant powder in methanol (1:3) for 24 h with occasional sonication at room temperature. A filter paper was used to filter the marc, and the entire process was repeated thrice. The filtrates were combined and concentrated using a rotary evaporator (Buchi Rotavapor R-200, Flawil, Switzerland) at 40 °C. The concentrated filtrate was stored at 4 °C in an airtight container until further use.

Fractionation and Re-Fractionation through CC. The crude extract was fractionated using solid-phase extraction. Silica gel 60 (70−230 mesh, Merck, Germany) was used as the stationary phase. The extract was adsorbed on silica and vacuum oven-dried at 45 °C. The solvents used for fractionation were *n*-hexanes, $CHCl_3$, and EtOAc. The volume of each solvent was decided based on the TLC banding pattern. The obtained fractions were concentrated using a rotary evaporator at 40 °C.

CC was used to process each fraction (*n*-hexanes, $CHCl_3$, and EtOAc) independently after adsorbing on silica gel and Sephadex LH-20 as per requirement. TLC analysis was used for the obtained aliquots and combined keeping in view the similarity in the bands. The 3rd fraction of E6 and 4th fraction of E8 were subjected to CC using Sephadex LH-20 with 1:1 ratio of EtAOc and MeOH to obtain the compounds. The entire process of fractionation and CC continued until prominent bioactivities of fractions or crystallization of compounds were achieved. The schematic flow sheet with the respective solvent system for each column is presented in Figure 1.

Phytochemical Analysis of Extracts. *Determination of Total Phenolic Contents.* Folin−Ciocalteu reagent was used to estimate the total phenolic contents (TPCs), as stated previously.[18] Initially, an aliquot of 20 μL (4 mg/mL extract in DMSO) was poured into a 96-well plate, followed by the addition of 90 μL of Folin−Ciocalteu reagent. The microplate was incubated for 5 min, and 90 μL of Na_2SO_4 solution was poured in the respective wells. The absorbance was measured at 630 nm using a microplate reader Elx 800 (BoiTek, USA). Gallic acid was used as the standard to plot a calibration curve ($y = 0.102x - 0.3048$; $R^2 = 0.9889$). The assay was performed in triplicate, and the results were expressed as micrograms of gallic acid equivalent per milligram extract (μg GAE/mg extract).

Determination of TFCs. Aluminum chloride colorimetric method was used to estimate the total flavonoid contents (TFCs) reported previously.[18] Samples of 20 μL (4 mg/mL extract in DMSO) were poured to each well, followed by the addition of 10 μL of aluminum chloride (10%). 10 μL of potassium acetate (1.0 M) and 160 μL of distilled water were added periodically to each well and mixed thoroughly. The 96-well microplate was incubated for 30 min at room temperature. The absorbance of the plate was recorded at 415 nm. Quercetin was used as the standard, and a calibration curve [$y = 0.0368x + 1.0954$ ($R^2 = 0.9872$)] was developed while the correlation was found to be significant at 0.05. The assay was run in triplicate, and results were expressed as micrograms of quercetin equivalent per milligram extract (μg QE/mg extract).

Radical Scavenging Activity−−DPPH Assay. The scavenging tendency of the tested samples was estimated using DPPH, as stated by Ali et al.[18] An aliquot of fractions and re-fractions of 10 μL was transferred to a 96-well plate, followed by the addition of 190 μL of DPPH solution. The microplate was later incubated for 30 min at 37 °C. The percent radical scavenging capacity (% RSA) was measured using spectrophotometric analysis, and the respective % inhibition (scavenging) concentration (SC_{50}) was described. Values above 50% were considered significant. The assay was performed in triplicate, and ascorbic acid was used as the standard. Percent radical scavenging activity (% inhibition) was calculated using the following equation

$$\text{percent radical scavenging capacity} = (1 - \text{Abs}/\text{Abc}) \times 100$$

where Abs is the absorbance of the DPPH solution with the tested sample, and Abc indicates the absorbance of the negative control (containing only the reagent).

Estimation of TAC. TAC reagent was used to determine the total antioxidant capacity (TAC) of fractions and re-fractions, as previously described.[18] Briefly, 100 μL of each fraction and re-fraction (4 mg/mL extract in DMSO) and positive and negative controls (ascorbic acid, 1 mg/mL) was mixed with 900 μL of the TAC reagent solution consisting of 0.6 M sulfuric acid, 28 mM sodium phosphate, and 4 mM ammonium molybdate. The reaction mixtures were kept in a water bath at 95 °C for 90 min and afterward cooled at room temperature. An aliquot of 200 μL of each tested sample was transferred to a microplate for spectrophotometric analysis at 630 nm using a microplate reader. Ascorbic acid was used as the standard, and a calibration curve ($y = 0.0212x + 0.0926$, $R^2 = 0.9913$) was plotted. The assay was performed in triplicate, and the results of antioxidant

https://doi.org/10.1021/acsomega.1c05647
ACS Omega 2022, 7, 3407−3423

capacity were expressed as micrograms of ascorbic acid equivalent per milligram (μg AAE/mg) of extract.

Estimation of the Total Reducing Power. Potassium ferricyanide colorimetric method was used to estimate the total reducing power (TRP) of fractions and re-fractions, as stated by Ali et al.[18] Initially, 200 μL of each tested sample (4 mg/mL extract in DMSO) was mixed with 400 μL of phosphate buffer (0.2 mol/L, pH 6.6) and 1% potassium ferricyanide [$K_3Fe(CN)_6$]. The mixture was incubated for 20 min at 50 °C. Trichloroacetic acid (400 μL of 10%) was added to the mixture and centrifuged at room temperature for 10 min at 3000 rpm. An aliquot of 200 μL of the upper layer of the centrifuged solution was transferred to a microplate and then ferric chloride (50 μL, 0.1%) was added to stop the reaction. The absorbance was measured at 630 nm. A calibration curve ($y = 0.038x + 0.7484$; $R^2 = 0.9967$) was plotted using ascorbic acid as a standard. The entire assay was performed in triplicate, and the results of reducing power were expressed as micrograms of ascorbic acid equivalent per milligram (μg AAE/mg) of extract.

Enzyme Inhibition Assays. *α-Amylase Inhibition Assay.* The fractions and subfractions were investigated for α-amylase inhibition potential in accordance to the procedure described previously.[18] Briefly, 15 μL of phosphate buffer (pH 6.8) was drained into a 96-well plate; later, 25 μL of α-amylase enzyme (0.14 U/mL), 10 μL of fractions and re-fractions (4 mg/mL in DMSO), and 40 μL of starch solution (2 mg/mL in potassium phosphate buffer) were added periodically. Incubation of samples was done for 30 min at 50 °C. Thereupon, 20 μL of 1 M HCl and, lastly, 90 μL of iodine reagent (5 mM iodine and 5 mM potassium iodide) were combined to the respective wells. The negative control represented 100% enzyme activity and contained no test sample. Acarbose was employed as a positive control, with the concentration range of 5−200 μg/mL. A well without the test sample and enzyme represented the blank. The results were obtained at 540 nm and were measured using a microplate reader. The percent α-amylase inhibition of the test samples was calculated using the following equation

$$\% \text{ enzyme inhibition} = \mathrm{OD(s)} - \mathrm{OD(n)} \div \mathrm{OD(b)} \times 100$$

where OD(s) = absorbance reading of the test sample; OD(n) = absorbance of the negative control; and OD(b) = absorbance of the blank.

Lipase Inhibition Assay. Lipase inhibition assay of test samples was investigated according to the described protocol with slight modifications.[18] Initially, lipase was dissolved in ultrapure water (10 mg/mL), and the supernatant was used after centrifugation for 5 min at 16,000 rpm. Tris buffer (100 mM; pH 8.2) was used as an assay buffer. Olive oil acted as a substrate (0.08% v/v dissolved in 5 mM sodium acetate, pH 5.0) containing 1% Triton X-100, heated in boiling water for 1 min to aid dissolution, and later cooled at room temperature. Each aliquot contained 350 μL of buffer, 150 μL of lipase, and 50 μL of test sample (4 mg/mL in DMSO); later, 450 μL of the substrate was added to initiate the reaction. Orlistat was used as a standard inhibitor, and Eppendorf without any test sample was considered as a blank. All the samples were incubated for 2 h at 37 °C. The test samples were centrifuged for 1 min at 16,000 rpm. Afterward, 200 μL was poured in the respective wells of the microplate. Absorbance was measured at 400 nm using a UV spectrophotometer. Results were compared with a standard inhibitor (Orlistat). The reaction's percent lipase inhibition was calculated using the following equation

$$\% \text{ enzyme inhibition} = \mathrm{OD(b)} - \mathrm{OD(s)} \div \mathrm{OD(b)} \times 100$$

where OD(b) = absorbance value of the blank and OD(s) = absorbance of the test sample.

Urease Inhibition Assay. The reaction mixture containing 25 μL of urease, 50 μL of phosphate buffer (3 mM, pH 4.5 containing 100 mM urea), and 10 μL of test samples (4 mg/mL in DMSO) was incubated for 15 min at 30 °C in a microplate. Subsequently, 45 μL of phenol reagent [1% (w/v) phenol and 0.005% (w/v) sodium nitroprusside] and 70 μL of alkali reagent [0.5% (w/v) NaOH and 0.1% NaOCl] were added to each well. Urease inhibition activity was measured to determine ammonia production that was evident with the pungent ammonia smell, as described by Ali et al.[18] The plates were incubated at 30 °C for 50 min, and the absorbance was measured at 630 nm using a UV spectrophotometer. Thiourea acted as a urease inhibitor and was considered as a control. The blank was prepared without any test sample. The control consisted of 60 μL of buffer rather than 50 μL, and the rest remained the same.

The reaction's percent urease inhibition was calculated using the following formula

$$\% \text{ enzyme inhibition} = \mathrm{OD(b)} - \mathrm{OD(s)} \div \mathrm{OD(b)} \times 100$$

where: OD(b) = absorbance value of the blank and OD(s) = absorbance of the test sample.

Toxicity Assays. *Brine Shrimp Lethality Assay.* A lethality test of 24 h was performed in a microplate against brine shrimp (*A. salina*) larvae as per the methodology stated earlier.[18] Eggs of *A. salina* (Ocean90, USA) were maintained for 24−48 h hatching period in simulated seawater (38 g/L supplemented with 6 mg/L dried yeast) in a specially designed two-compartment tray with constant oxygen supply under illumination. Pasteur pipette was used to harvest the mature phototropic nauplii and restationed to each well of the microplate. The corresponding volume of the test samples containing DMSO ≤1% in seawater with the final concentrations of 200, 100, 50, and 25 μg/mL was transferred to each corresponding well. Positive and negative control wells consisted of standard doxorubicin (4 mg/mL) and 1% DMSO in seawater, respectively. After 24 h, the degree of lethality exhibited by each fraction and re-fraction was determined by counting the number of survivors and the median lethal concentration (LC_{50}) of the test samples with mortality ≥50%, using the table curve 2D v5.01 software. The entire experiment was performed in triplicate.

Protein Kinase Inhibition Assay. The purified isolates of *Streptomyces 85E* strain were used to perform protein kinase inhibition assay by observing hyphae formation.[18] The minimal ISP4 media was used to develop bacterial lawn using refreshed culture of *Streptomyces* on sterile plates by spreading spores (mycelia fragments). About 5 μL of each fraction and re-fraction (20 mg/mL extract in DMSO) was loaded on sterile 6 mm filter paper discs and placed directly on the *Streptomyces 85E*-seeded plates. For positive and negative controls, surfactin and DMSO-infused discs were used, respectively. The plates were then incubated for 72 h at 30 °C, and the results were interpreted measuring bald ZOI around the tested samples and control-infused discs.

Antimicrobial Assays. *Antibacterial Assay.* Disc diffusion method was used to determine the antibacterial potential of the fractions and re-fractions, as stated earlier.[18] Two Gram-positive bacterial strains, *S. aureus* (ATCC # 6538) and *B. subtilis* (ATCC # 6633), and three Gram-negative bacterial strains, *E.*

https://doi.org/10.1021/acsomega.1c05647
ACS Omega 2022, 7, 3407−3423

coli (ATCC 15224), *P. aeruginosa* (ATCC # 9721), and *K. pneumoniae* (ATCC # 4619), with accustomed seeding density were inoculated on nutrient agar plates. Sterile filter paper discs permeated with 5 μL (20 mg/mL extract in DMSO) of fractions and re-fractions were placed on the seeded plates. Roxithromycin acted as a positive control, while DMSO-infused disc was used as a negative control. The test samples were incubated for 24 h at 37 °C, and an average diameter of clear ZOI around the sample and the control-infused discs was measured. The test was performed in triplicate.

Antifungal Assay. The antifungal tendency of the fractions and re-fractions was measured in triplicate analysis using the disc diffusion method.[18] The fungal spores of strains [*F. solani* (FCBP # 0291), *Mucor* species (FCBP # 0300), *A. niger* (FCBP # 0198), *A. fumigatus* (FCBP # 66), and *A. flavus* (FCBP # 0064)] were amassed in 0.02%, Tween 20 solution, and their turbidity was adjusted according to the McFarland 0.5 turbidity standard. A 100 μL of harvested fungal strain was swabbed on plates containing Sabouraud dextrose agar. A filter paper disc impregnated with 5 μL (20 mg/mL extract in DMSO) of test samples was placed directly on the inoculated plates. For negative control, DMSO-impregnated disc was used, whereas for positive control clotrimazole was used. The plates were incubated for 24−48 h at 28 °C, and an average diameter (mm) of the zone of growth inhibition around the discs impregnated with test samples and the control was measured and recorded.

Characterization of Compounds Isolated Using CC. Compound **1** (lupeol) was isolated from the H8 fraction (AM-6), 8th fraction of 1−8 of H1−H16 of *n*-hexane fractionation (AM-7), 3rd fraction of 1−12 of C5−C6 of chloroform fractionation (AM-8), and from the E3 fraction of ethyl acetate fractionation (EM-5 and EM-8). Compound **2** (AM-5 as 1-triacontanol) was crystallized in the H3 fraction of *n*-hexane fractionation. Compound **3** (EM-6 as methyl benzoate) was separated from the 4th fraction of 7−10 of E1−E10 of ethyl acetate fractionation. Compound **4** (EM-11 as benzoic acid) was obtained after the fractionation of the 3rd fraction of E6 fraction using CC and Sephadex LH-20 as the stationary phase, and compound **5** (EM-9 as ursolic acid) was obtained similarly by using Sephadex LH-20 to fractionate the 4th fraction of E8 to retrieve an active component. Compound **6** (EM-7 as 3-hydroxybenzoic acid) was obtained similarly by using Sephadex LH-20 to fractionate the 3rd fraction of E8 to retrieve an active component (Figure 1). The NMR spectra were recorded by using a Bruker AMX-400 spectrometer (^{1}H NMR at 400 MHz and ^{13}C NMR at 100 MHz). A Varian MAT-312 spectrometer was used to record HR-EI-MS.

3β-Lup-20(29)-en-3-ol (Lupeol). mp 213.8−215.2 °C. IR (KBr, cm^{-1}): 3400, 2920, 1640, 1470, 1140. ^{1}H NMR ($CDCl_3$, 400 MHz): δ 4.70 (1H, s, H-29a), 4.59 (1H, s, H-29b), 3.20 (1H, dd, J = 11.2, 5.0 Hz, H-3), 2.40 (1H, m, H-19), 1.70 (3H, s, CH_3-29), 1.05 (3H, s, CH_3-26), 1.00 (3H, s, CH_3-23),, 0.97 (3H, s, CH_3-27), 0.85 (3H, s, CH_3-25),, 0.81 (3H, s, CH_3-24),, 0.78 (3H, s, CH_3-26); ^{13}C NMR ($CDCl_3$, 100 MHz): δ 38.06 (C-1), 27.43 (C-2), 79.03 (C-3), 38.71 (C-4), 55.30 (C-5), 18.33 (C-6), 34.29 (C-7), 40.84 (C-8), 50.45 (C-9), 37.18 (C-10), 20.94 (C-11), 25.15 (C-12), 38.87 (C-13), 42.84 (C-14), 27.46 (C-15), 35.59 (C-16), 43.01 (C-17), 48.31 (C-18), 48.00 (C-19), 151.01 (C-20), 29.86 (C-21), 40.01 (C-22), 28.00 (C-23), 15.38 (C-24), 16.13 (C-25), 15.98 (C-26), 14.56 (C-27), 18.01 (C-28), 109.33 (C-29), 19.31 (C-30); HREIMS m/z: $[M]^+$ 426.3880 calcd for $C_{30}H_{50}O$; 426.3861.

1-Triacontanol. Colorless needles (18 mg); mp 87−89 °C; IR (KBr): 3395, 2955, 1116 cm^{-1}; ^{1}H NMR (400 MHz, $CDCl_3$): δ 3.62 (2H, t, J = 6.8 Hz, H-1), 1.52 (2H, m, H-2), 1.23 (55H, br s, H-3-29), 0.86 (3H, t, J = 6.8 Hz, H-31); ^{13}C NMR (100 MHz, $CDCl_3$): δ 63.1 (C-1), 32.8−29.4 (C-3-29), 25.8 (C-2), 22.7 (C-30), 14.1 (C-31); HREIMS m/z: $[M]^+$ 452.4820 (calcd for $C_{30}H_{62}O$; 438.4800).

Methyl Benzoate. Colorless liquid; bp: 199−200 °C; UV (CD_3OD) λ_{max} log ε: 229, 273, 301 nm; IR (KBr) ν_{max} cm^{-1}: 1755 (C═O), 1620−1499 (Ar C═C), 1165 (C−O); ^{1}H NMR ($CDCl_3$, 400 MHz): δ 8.10 (2H, d, J = 8.5 Hz, H-2,6), 7.61 (1H, t, J = 8.5 Hz, H-4), 7.45 (2H, t, J = 8.5 Hz, H-3,5), 3.80 (3H, s, OCH_3); ^{13}C NMR (CD_3OD, 100 MHz): δ 168.3 (C-7), 135.4 (C-4), 131.7 (C-1), 130.6 (C-2,6), 129.9 (C-3,5), 56.8 (OCH_3); HREIMS m/z: $[M]^+$ 136.0544 (calcd for $C_8H_8O_2$, 136.0524).

Benzoic Acid. Colorless needles; mp 120−122 °C; UV (CD_3OD) λ_{max} log ε: 228, 272, 300 nm; IR (KBr) ν_{max} cm^{-1}: 3260−2610 (COOH), 1696 (C═O), 1626−1494 (Ar C═C); ^{1}H NMR ($CDCl_3$, 400 MHz): δ 11.92 (1H, br s, COOH), 8.12 (2H, d, J = 8.5 Hz, H-2,6), 7.60 (1H, t, J = 8.5 Hz, H-4), 7.46 (2H, t, J = 8.5 Hz, H-3,5); ^{13}C NMR (CD_3OD, 100 MHz): δ 173.0 (C-7), 134.5 (C-4), 131.1 (C-1), 130.7 (C-2,6), 129.7 (C-3,5); HREIMS m/z: $[M]^+$ 122.0387 (calcd for $C_7H_6O_2$, 122.0367).

Ursolic Acid. Colorless amorphous powder (18 mg); mp 283−285 °C; IR (KBr): 3435, 3019, 2927, 1643, 1528, 1216 cm^{-1}; ^{1}H NMR (400 MHz, $CDCl_3$): δ 5.23 (1H, t, J = 5.6 Hz, H-12), 3.25 (1H, dd, J = 11.5, 5.2 H-3), 1.19 (3H, s, Me-27), 0.97 (3H, s, Me-23), 0.93 (3H, s, Me-25), 0.89 (3H, s, Me-26), 0.87 (3H, d, J = 7.1 Hz, Me-30), 0.84 (3H, d, J = 7.1 Hz, Me-29), 0.76 (3H, s, Me-24); ^{13}C NMR (100 MHz, $CDCl_3$): δ 179.6 (C-28), 138.9 (C-13), 125.1 (C-12), 78.8 (C-3), 55.2 (C-18), 52.4 (C-5), 47.9 (C-17), 47.4 (C-9), 42.0 (C-14), 39.6 (C-8), 38.5 (C-1), 37.0 (C-22), 37.1 (C-10), 33.2 (C-7), 30.5 (C-19), 30.3 (C-20), 29.4 (C-15), 27.5 (C-21), 24.5 (C-27), 27.4 (C-2), 24.0 (C-23, C-30), 23.9 (C-11), 23.5 (C-16), 22.4 (C-29), 18.3 (C-6), 17.2 (C-26), 15.9 (C-25), 15.4 (C-24); HREIMS m/z: $[M]^+$ 456.3620 (calcd for $C_{30}H_{48}O_3$; 456.3603).

3-Hydroxybenzoic Acid. Colorless crystalline solid; mp 201−203 °C; UV (CD_3OD) λ_{max} log ε: 232, 277, 304 nm; IR (KBr) ν_{max} cm^{-1}: 3255−2615 (COOH), 1692 (C═O), 1626−1494 (Ar C═C), 1165 (C−O); ^{1}H NMR ($CDCl_3$, 400 MHz): δ 11.85 (1H, br s, COOH), 7.43 (1H, s, H-2), 7.36 (1H, d, J = 8.5 Hz, H-6), 7.30 (1H, t, J = 8.5 Hz, H-5), 7.02 (1H, t, J = 8.5 Hz, H-4); ^{13}C NMR (CD_3OD, 100 MHz): δ 170.3 (C-7), 157.4 (C-3), 132.2 (C-1), 129.6 (C-5), 120.1 (C-2), 115.9 (C-4); HREIMS m/z: $[M]^+$ 138.0336 (calcd for $C_7H_6O_3$, 138.0316).

Statistical Analysis. All the antioxidant, enzymatic, and phytochemical experiments were performed in triplicate. The data are presented as mean ± standard deviation. LC_{50} was calculated by the table curve 2D Ver.4 software.

AUTHOR INFORMATION

Corresponding Author

Muhammad Zia − *Department of Biotechnology, Quaid-i-Azam University Islamabad, Islamabad 45320, Pakistan;* orcid.org/0000-0002-4878-6810; Phone: +925190644126; Email: ziachaudhary@gmail.com

Authors

Joham Sarfraz Ali − *Department of Biotechnology, Quaid-i-Azam University Islamabad, Islamabad 45320, Pakistan*

https://doi.org/10.1021/acsomega.1c05647
ACS Omega 2022, 7, 3407−3423

Naheed Riaz − *Institute of Chemistry, The Islamia University of Bahawalpur, Bahawalpur 63100, Pakistan*
Abdul Mannan − *Department of Pharmacy, COMSATS University, Abbottabad Campus, Abbottabad 22060, Pakistan*
Saira Tabassum − *Department of Biotechnology, Quaid-i-Azam University Islamabad, Islamabad 45320, Pakistan*

Complete contact information is available at:
https://pubs.acs.org/10.1021/acsomega.1c05647

Funding

The research work was funded by Higher Education Commission, Pakistan, under the Indigenous PhD Fellowship program to J.S.A.

Notes

The authors declare no competing financial interest.

REFERENCES

(1) Rauf, A.; Khalique, A. Unani Herbal Drugs: A Ray of Hope for the Management of Diabetes Mellitus. *J. Integ. Comm. Health* **2019**, *8*, 21−26.
(2) Bernhoft, A. A brief review on bioactive compounds in plants. *Bioactive compounds in plants-benefits and risks for man and animals* **2010**, *50*, 11−17.
(3) Fatima, H.; Khan, K.; Zia, M.; Ur-Rehman, T.; Mirza, B.; Haq, I. U. Extraction optimization of medicinally important metabolites from Datura innoxia Mill.: an in vitro biological and phytochemical investigation. *BMC Complementary Altern. Med.* **2015**, *15*, 376.
(4) Brusotti, G.; Cesari, I.; Dentamaro, A.; Caccialanza, G.; Massolini, G. Isolation and characterization of bioactive compounds from plant resources: the role of analysis in the ethnopharmacological approach. *J. Pharm. Biomed. Anal.* **2014**, *87*, 218−228.
(5) Wink, M. Introduction: Biochemistry, Physiology and Ecological Functions of Secondary Metabolites. *Annual Plant Reviews Volume 39: Functions and Biotechnology of Plant Secondary Metabolites*; John Wiley & Sons, Ltd., 2010; pp 1−20.
(6) Moteriya, P.; Satasiya, R.; Chanda, S. Screening of phytochemical constituents in some ornamental flowers of Saurashtra region. *J. Pharmacogn. Phytochem.* **2015**, *3*, 112−120.
(7) Sisay, M.; Bussa, N.; Gashaw, T.; Mengistu, G. Investigating in vitro antibacterial activities of medicinal plants having folkloric repute in ethiopian traditional medicine. *J. Evidence-Based Integr. Med.* **2019**, *24*, 2515690X19886276.
(8) Weller, M. G. A unifying review of bioassay-guided fractionation, effect-directed analysis and related techniques. *Sensors* **2012**, *12*, 9181−9209.
(9) Ali, J. S.; Khan, I.; Zia, M. Antimicrobial, cytotoxic, phytochemical and biological properties of crude extract and solid phase fractions of Monotheca buxifolia. *Adv. Tradit. Med.* **2020**, *20*, 115−122.
(10) Murad, W.; Azizullah, A.; Adnan, M.; Tariq, A.; Khan, K. U.; Waheed, S.; Ahmad, A. Ethnobotanical assessment of plant resources of Banda Daud Shah, district Karak, Pakistan. *J. Ethnobiol. Ethnomed.* **2013**, *9*, 77.
(11) Jan, S.; Khan, M. R.; Rashid, U.; Bokhari, J. Assessment of antioxidant potential, total phenolics and flavonoids of different solvent fractions of Monotheca buxifolia fruit. *Osong Public Health Res. Perspec.* **2013**, *4*, 246−254.
(12) Rehman, J.; Khan, I. U.; Farid, S.; Kamal, S.; Aslam, N. Phytochemical screening and evaluation of in-vitro antioxidant potential of Monotheca buxifolia. *E3 J. Biotechnol. Pharm. Res.* **2013**, *4*, 54−60.
(13) Ullah, I.; Khan, J. A.; Shahid, M.; Khan, A.; Adhikari, A.; Hannan, P. A.; Farooq, U. Pharmacological screening of Monotheca buxifolia (Falc.) A. DC. for antinociceptive, anti-inflammatory and antipyretic activities. *BMC Complementary Altern. Med.* **2016**, *16*, 273.
(14) Burki, S.; Mehjabeen; Burki, Z. G.; Shah, Z. A.; Imran, M.; Khan, M. Phytochemical screening, antioxidant and in vivo neuropharmacological effect of Monotheca buxifolia (Falc.) barks extract. *Pak. J. Pharm. Sci.* **2018**, *31*, 1519.
(15) Jan, S.; Khan, M. R. Protective effects of Monotheca buxifolia fruit on renal toxicity induced by CCl 4 in rats. *BMC Complementary Altern. Med.* **2016**, *16*, 289.
(16) Hazrat, A.; Nisar, M.; Zaman, S. Antibacterial activities of sixteen species of medicinal plants reported from Dir Kohistan Valley KPK, Pakistan. *Pak. J. Bot.* **2013**, *4515*, 1369−1374.
(17) Ali, J. S.; Saleem, H.; Mannan, A.; Zengin, G.; Mahomoodally, M. F.; Locatelli, M.; Zia, M. Metabolic fingerprinting, antioxidant characterization, and enzyme-inhibitory response of Monotheca buxifolia (Falc.) A. DC. extracts. *BMC Complementary Med. Ther.* **2020**, *20*, 313.
(18) Ali, J. S.; Riaz, N.; Mannan, A.; Latif, M.; Zia, M. Antioxidant, antimicrobial, enzyme inhibition, and cytotoxicity guided investigation of Sideroxylon mascatense (A. DC.) TD Penn. leaves extracts. *Nat. Prod. Res.* **2021**, 1−4.
(19) Khan, I.; Ali, J. S.; Ul-Haq, I.; Zia, M. Biological and phytochemicals properties of Monotheca buxifolia: an unexplored medicinal plant. *Pharm. Chem. J.* **2020**, *54*, 293−301.
(20) Kanagavalli, U.; Sadiq, M.; Priya, L.; Shobana, R. The comparative preliminary phytochemical investigation, TLC analysis and antioxidant activity of different solvent extracts of Boerhavia diffusa Linn. *Int. J. Res. Pharm. Sci.* **2019**, *10*, 245−256.
(21) Lim, S. M.; Agatonovic-Kustrin, S.; Lim, F. T.; Ramasamy, K. High-performance thin layer chromatography-based phytochemical and bioactivity characterisation of anticancer endophytic fungal extracts derived from marine plants. *J. Pharm. Biomed. Anal.* **2021**, *193*, 113702.
(22) Kumar, S.; Chashoo, G.; Saxena, A. K.; Pandey, A. K. Parthenium Hysterophorus: A Probable Source of Anticancer, Antioxidant and Anti-HIV Agents. *Biomed Res. Inter.* **2013**, *2013*, 810734.
(23) Afshar, F. H.; Delazar, A.; Nazemiyeh, H.; Esnaashari, S.; Moghadam, S. B. Comparison of the total phenol, flavonoid contents and antioxidant activity of methanolic extracts of Artemisia spicigera and A. splendens growing in Iran. *Pharm. Sci.* **2012**, *18*, 165−170.
(24) Murad, M.; Aminah, A.; Wan Aida, W. M. Total phenolic content and antioxidant activity of kesum (Polygonum minus), ginger (Zingiber officinale) and turmeric (Curcuma longa) extract. *Int. Food Res. J.* **2011**, *18*, 45.
(25) Kumar, V.; Malhotra, S. V. Synthesis of nucleoside-based antiviral drugs in ionic liquids. *Bioorg. Med. Chem. Lett.* **2008**, *18*, 5640−5642.
(26) Mouderas, F.; El Haci, I. A.; Lahfa, F. B. Phytochemical profile, antioxidant and antimicrobial activities of Traganum nudatum Delile aerial parts organic extracts collected from Algerian Sahara's flora. *Orient. Pharm. Exp. Med.* **2019**, *19*, 299−310.
(27) Gourine, N.; Yousfi, M.; Bombarda, I.; Nadjemi, B.; Stocker, P.; Gaydou, E. M. Antioxidant activities and chemical composition of essential oil of Pistacia atlantica from Algeria. *Ind. Crops Prod.* **2010**, *31*, 203−208.
(28) Nickavar, B.; Yousefian, N. Evaluation of α-amylase inhibitory activities of selected antidiabetic medicinal plants. *J. Verbraucherschutz Lebensmittelsicherh.* **2011**, *6*, 191−195.
(29) Wickramaratne, M. N.; Punchihewa, J. C.; Wickramaratne, D. B. M. In vitro alpha amylase inhibitory activity of the leaf extracts of Adenanthera pavonina. *BMC Complementary Altern. Med.* **2016**, *16*, 466.
(30) Yao, G.; Sebisubi, F. M.; Voo, L. Y. C.; Ho, C. C.; Tan, G. T.; Chang, L. C. Citrinin derivatives from the soil filamentous fungus Penicillium sp. H9318. *J. Braz. Chem. Soc.* **2011**, *22*, 1125−1129.
(31) Waters, B.; Saxena, G.; Wanggui, Y.; Kau, D.; Wrigley, S.; Stokes, R.; Davies, J. Identifying protein kinase inhibitors using an assay based on inhibition of aerial hyphae formation in Streptomyces. *J. Antibiot.* **2002**, *55*, 407−416.
(32) M Nguta, J.; Mbaria, J. M.; Gakuya, D. W.; Gathumbi, P. K.; Kabasa, J. D.; Kiama, S. G. Evaluation of acute toxicity of crude plant extracts from kenyan biodi-versity using brine shrimp, artemia salina l. (artemiidae). *Open Conf. Proc. J.* **2012**, *3*, 30−34.

(33) Kaushik, P.; Goyal, P. In vitro evaluation of Datura innoxia (thorn-apple) for potential antibacterial activity. *Indian J. Microbiol.* **2008**, *48*, 353.
(34) Cueva, C.; Moreno-Arribas, M. V.; Martín-Álvarez, P. J.; Bills, G.; Vicente, M. F.; Basilio, A.; Rivas, C. L.; Requena, T.; Rodríguez, J. M.; Bartolomé, B. Antimicrobial activity of phenolic acids against commensal, probiotic and pathogenic bacteria. *Res. Microbiol.* **2010**, *161*, 372−382.
(35) Lagrouh, F.; Dakka, N.; Bakri, Y. The antifungal activity of Moroccan plants and the mechanism of action of secondary metabolites from plants. *J. Mycol. Med.* **2017**, *27*, 303−311.
(36) Burns, D.; Reynolds, W. F.; Buchanan, G.; Reese, P. B.; Enriquez, R. G. Assignment of 1H and 13C spectra and investigation of hindered side-chain rotation in lupeol derivatives. *Magn. Reson. Chem.* **2000**, *38*, 488−493.
(37) Liu, J. Pharmacology of oleanolic acid and ursolic acid. *Journal of ethnopharmacology* **1995**, *49* (2), 57−68.
(38) Hamzah, A. S.; Lajis, N. H. Chemical constituents of Hedyotis herbacea. *ASEAN Rev. Biodivers. Environ. Conserv.* **1998**, *2*, 1−6.
(39) Násfay Scott, K. NMR parameters of biologically important aromatic acids I. Benzoic acid and derivatives. *J. Magn. Reson.* **1970**, *2*, 361−376.
(40) Shai, L. J.; McGaw, L. J.; Aderogba, M. A.; Mdee, L. K.; Eloff, J. N. Four pentacyclic triterpenoids with antifungal and antibacterial activity from Curtisia dentata (Burm.f) C.A. Sm. leaves. *J. Ethnopharmacol.* **2008**, *119*, 238−244.
(41) Mathabe, M. C.; Hussein, A. A.; Nikolova, R. V.; Basson, A. E.; Meyer, J. J. M.; Lall, N. Antibacterial activities and cytotoxicity of terpenoids isolated from Spirostachys africana. *J. Ethnopharmacol.* **2008**, *116*, 194−197.
(42) Kuiate, J.-R.; Mouokeu, S.; Wabo, H. K.; Tane, P. Antidermatophytic triterpenoids fromSyzygium jambos (L.) Alston (Myrtaceae). *Phytother. Res.* **2007**, *21*, 149−152.
(43) Bi, Y.; Xu, J.; Wu, X.; Ye, W.; Yuan, S.; Zhang, L. Synthesis and cytotoxic activity of 17-carboxylic acid modified 23-hydroxy betulinic acid ester derivatives. *Bioorg. Med. Chem. Lett.* **2007**, *17*, 1475−1478.
(44) Rajendran, P.; Jaggi, M.; Singh, M. K.; Mukherjee, R.; Burman, A. C. Pharmacological evaluation of C-3 modified Betulinic acid derivatives with potent anticancer activity. *Invest. New Drugs* **2008**, *26*, 25−34.
(45) Mostafiz, M. M.; Alam, M. B.; Chi, H.; Hassan, E.; Shim, J.-K.; Lee, K.-Y. Effects of Sublethal doses of methyl benzoate on the life history traits and acetylcholinesterase (AChE) activity of Aphis gossypii. *Agronomy* **2020**, *10*, 1313.
(46) Feng, Y.; Zhang, A. A floral fragrance, methyl benzoate, is an efficient green pesticide. *Sci. Rep.* **2017**, *7*, 42168.
(47) Ikeda, Y.; Murakami, A.; Ohigashi, H. Ursolic acid: An anti- and pro-inflammatory triterpenoid. *Mol. Nutr. Food Res.* **2008**, *52*, 26−42.
(48) Son, J.; Lee, S. Y. Therapeutic potential of ursonic acid: Comparison with ursolic acid. *Biomolecules* **2020**, *10*, 1505.

https://doi.org/10.1021/acsomega.1c05647
ACS Omega 2022, 7, 3407−3423